Atti Soc. tosc. Sci. nat., Mem., Serie A, 102 (1995)
pagg. 21-38, figg. 8, tabb. 8

C. ROMBAI, T. TRUA, M. MATTEINI

METAMORPHIC XENOLITHS AND MAGMATIC INCLUSIONS IN THE QUATERNARY LAVAS OF MT. AMIATA (TUSCANY, CENTRAL ITALY): INFERENCES FOR P-T CONDITIONS OF MAGMA CHAMBER

Abstract - New chemical and mineralogical data on volcanics, magmatic inclusions and metamorphic xenoliths of Mount Amiata (MA) (southern Tuscany, Italy) are here reported. The MA volcanic products have been distinguished in: Basal Trachydacite (BT), Trachydacitic Domes (TD), Late Trachydacites (LT) and Final Latites (FL). The BT, TD and LT show a subalkaline affinity and belong to the shoshonitic serie, whereas FL and magmatic inclusions have chemical features typical of ultrapotassic basic rocks. Plagioclase, sanidine, biotite, ortho- and clinopyroxenes are common phases in these volcanics. Olivine crystals only occur in the TD and FL; resorbed quartz is present in the BT and FL. The magmatic inclusions are rich in biotites and pyroxenes, whereas the amount of the other phases (plagioclase, sanidine and ilmenite) is variable. Microprobe analyses have been carried out on 3 TD, 1 FL and 2 magmatic inclusions. Olivine has Fo_{85-40} contents. Plagioclase is An_{87-47} in the MA volcanics and An_{61-54} in magmatic inclusions. Orthopyroxene has $Mg\#_{73-44}$ in the volcanics, and $Mg\#_{50}$ in magmatic inclusions, whereas clinopyroxene crystals show in all the samples diopsidic to augitic composition. Only in the most basic inclusion (AM170) clinopyroxene phenocrysts have oscillatory zoning with diopsidic to hedenbergitic composition. The chemical variations observed in the clinopyroxenes of volcanics and magmatic inclusions could be explained as due to variations of the T and P conditions of magma during the crystallization, whereas it seems that $f(O_2)$ does not play an important role. Moreover, the oscillatory zoning of the AM170 clinopyroxenes could be interpreted as due to inputs of more mafic magma in the magmatic chamber.
Among the eleven metamorphic xenoliths studied petrographically, three of these have been analysed by microprobe. According to their mineralogical assemblage, these xenoliths have been subdivided in three groups: *assemblage a*, made of plagioclase, sanidine, biotite, orthopyroxene, graphite and quartz; *assemblage b*, in which sillimanite, plagioclase, sanidine, biotite, corundum, spinel, cordierite and garnet occur; *assemblage c*, which is constituted of sanidine, plagioclase, biotite, spinel, orthopyroxene and glass. Coexisting garnet-sillimanite-spinel-cordierite-corundum in the AM38 sample and the Fe/Mg distributions between these phases allow to define the T-P conditions at which the MA magmatic chamber was emplaced.

Key words - Mount Amiata, metamorphic xenoliths, magmatic inclusions.

Riassunto - *Gli xenoliti metamorfici e gli inclusi magmatici nelle lave quaternarie del Mt. Amiata (Toscana, Italia centrale): supposizioni sulle condizioni di P-T della camera magmatica.* In questo lavoro sono riportati nuovi dati chimici e mineralogici sulle lave, sugli inclusi magmatici e sugli xenoliti metamorfici del Monte Amiata (MA) (Toscana meridionale, Italia). In accordo con le fasi eruttive i prodotti del MA sono stati suddivisi in: Trachidaciti Basali (BT), Duomi Trachidacitici (TD), Trachidaciti Finali (FT) e Latiti Finali (FL). Le BT, TD, FT mostrano un'affinita' subalcalina e appartengono alla serie shoshonitica, mentre le FL e gli inclusi magmatici hanno caratteristiche chimiche tipiche di rocce basiche alcaline ultrapotassiche. Nelle vulcaniti del MA plagioclasio, sanidino, orto- e clinopirosseno sono le fasi comuni. Cristalli di olivina si ritrovano nei TD e nelle FL, ed il quarzo riassorbito è presente solo nelle BT e nelle FL. Tutti gli inclusi magmatici sono ricchi in biotite e pirosseno e mostrano quantità variabili di plagioclasio, sanidino e ilmenite.
Analisi di fase mediante microsonda elettronica sono state effettuate su 3TD, 1FL e 2 inclusi magmatici. L'olivina varia da Fo_{85-40}. Il plagioclasio mostra variazioni composizionali sia nelle vulcaniti (An_{87-47}), che negli inclusi magmatici (An_{61-54}). Nelle vulcaniti e negli inclusi magmatici l'ortopirosseno ha rispettivamente $Mg\#_{44-73}$ ed $Mg\#_{50}$, mentre in entrambi il clinopirosseno ha composizione variabile da diopsidica ad augitica. Solo nell'incluso magmatico più basico (AM 170) i fenocristalli di clinopirosseno presentano zonature oscillanti con composizione da diopsidica a hedembergitica. Le variazioni chimiche osservate nei clinopirosseni delle vulcaniti e degli inclusi magmatici sono attribuite a variazioni nelle condizioni di P e T del magma, piuttosto che a variazioni della $f(O_2)$. Inoltre le zonature oscillatorie osservate nei clinopirosseni dell'incluso basico AM 170 possono essere considerate come testimoni di un ingresso di magma più basico nella camera magmatica.
Sono stati studiati petrograficamente 11 xenoliti metamorfici (su 3 campioni sono state eseguite analisi di fase in microsonda). In base alle loro associazioni mineralogiche sono stati suddivisi in tre gruppi: *associazione «a»*, costituita da plagioclasio, sanidino, biotite, ortopirosseno, grafite e quarzo; *associazione «b»*, nella quale ritroviamo sillimanite, plagioclasio, sanidino, biotite, corindone, spinello, cordierite e granato; *associazione «c»*, costituita da sanidino, plagioclasio, biotite, spinello, ortopirosseno e vetro. La coesistenza di granato-sillimanite-spinello-cordierite-corindone nell'incluso metamorfico AM 38 e la distribuzione Fe/Mg fra queste fasi permettono di risalire alle condizioni T-P alle quali si è impostata la camera magmatica.

Parole chiave - Monte Amiata, xenoliti metamorfici, inclusi magmatici.

Dipartimento di Scienze della Terra, Università di Pisa, Via S. Maria 53, Pisa, Italy.

INTRODUCTION

Two petrographic provinces represent the magmatism of the central Italy. They are known as: the Tuscan Magmatic Province («Provincia Magmatica Toscana», PMT) and the Roman Magmatic Province («Provincia Magmatica Romana», PMR) (Serri *et al.*, 1993) (Fig. 1). The Mount Amiata (MA) volcanic massif belongs to the PMT and it extends over an area of 85 Km^2, about 30 Km north of Vulsini, the northernmost Roman volcanic complex (Fig. 1). It represents the most recent volcanic event of the PMT (0.29-0.18 Ma; Bigazzi *et al.*, 1981) and it is the sole volcanic center of the PMT to be active within the age range of the northwestern PMR (0.63-0.05 Ma; Serri *et al.*, 1993). Four periods of main volcanic activity have been recognized for the MA volcanism (Mazzuoli and Pratesi, 1963; Van Bergen, 1985). During the first period dacitic lavas were outpoured from a faults system with a NNE-SSW direction about 10 Km long (Fig. 2). These lavas show typical structures of acid flows, with brecciated margins and dense tongues of lava among the breccia. The following activity was characterized by the emplacement of dacitic lava domes, aligned along the same faults system, and on fissures with a conjugate direction (Fig. 2). The third period of activity produced three acid lava flows outpoured from the flanks of two lava domes. The volcanism ends with the emis-

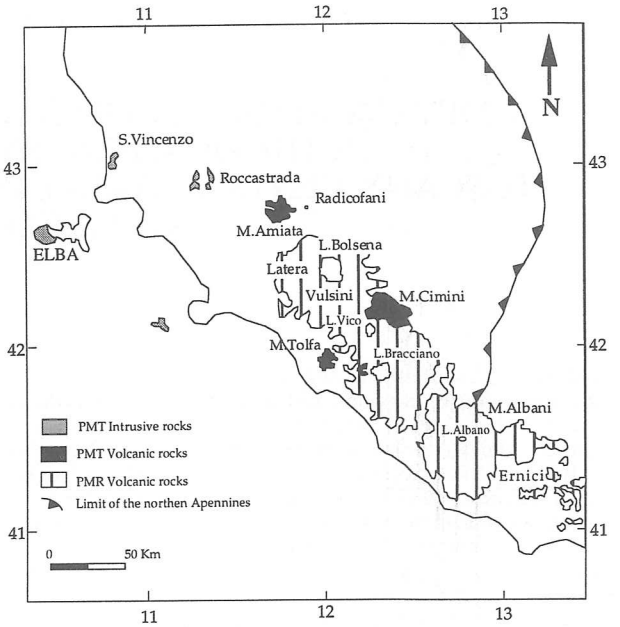

Fig. 1 - Schematic map of the magmatic rocks of the Tuscan Magmatic Province («Provincia Magmatica Toscana», PMT) and northwestern Roman Magmatic Province («Provincia Magmatica Romana», PMR) (modified from Innocenti *et al.*, 1992).

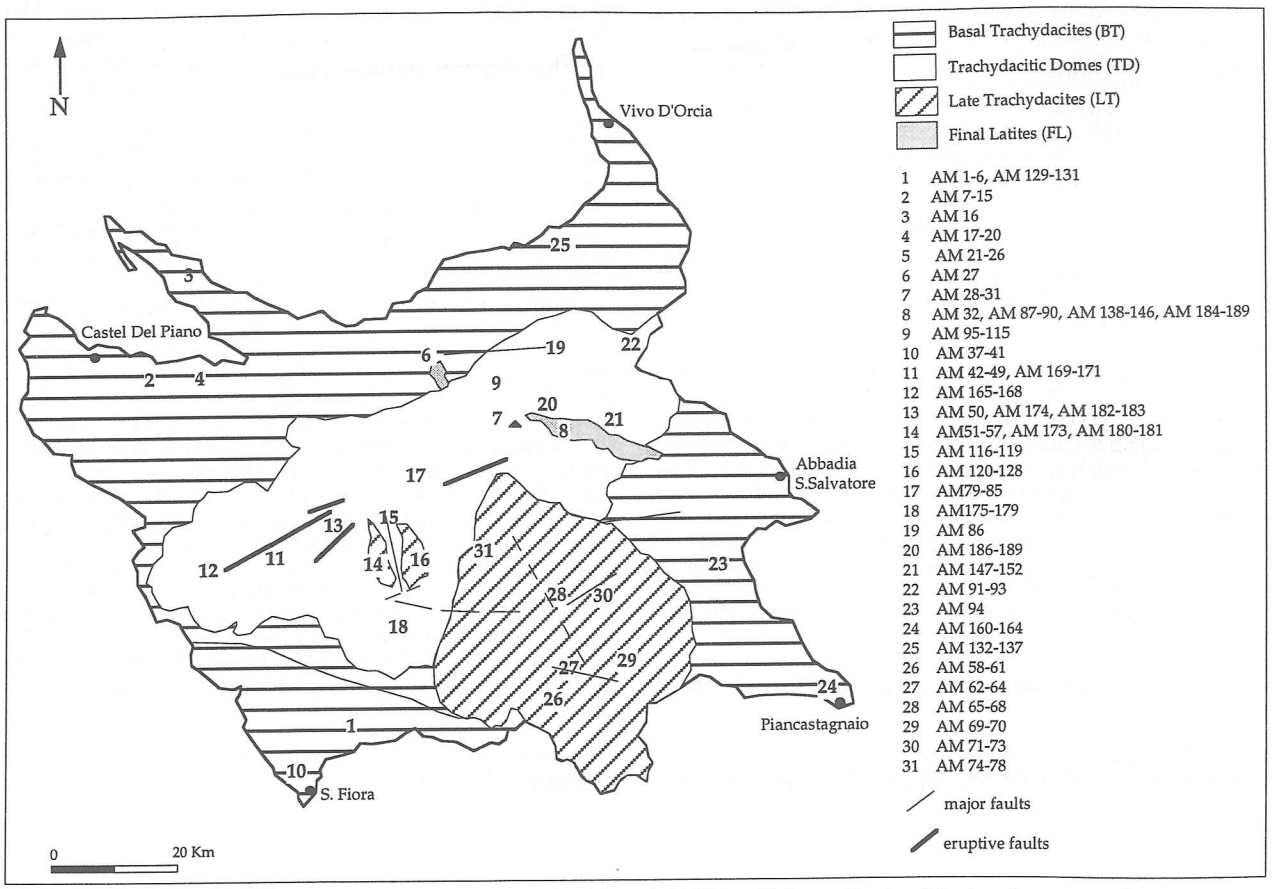

Fig. 2 - Geological map of Mt. Amiata (modified from Mazzuoli and Pratesi, 1963) in which sampling localities have been reported.

sion of two small latitic lava flows outpoured from the same NNE-SSW eruptive fault (Fig. 2).
The MA volcanism lasted a relatively short span of time. K/Ar and fission tracks measurements carried out on glasses, indicate ages ranging from 0.29 to 0.18 Ma (Bigazzi *et al.*, 1981). The chemical and Sr isotope characteristics of these volcanics are consistent with mixing between crustal-derived magma and mantle-derived magma (Van Bergen, 1985), the latter component being similar to lavas of the Roman high-K series (Poli *et al.*, 1984).
MA volcanics contain numerous metamorphic xenoliths and magmatic inclusion. The former are widespread in all the lavas, whereas the latter are concentrated in the lava domes and in the final lava flows. The metamorphic xenoliths have been interpreted as deriving from a contact aureole fragmented during the volcanic processes and uplifted by the viscous magma (Van Bergen, 1983; Van Bergen and Barton, 1984). The magmatic inclusions have been considered as hybrid inclusions derived by the injection of mafic magma into a siliceous magma chamber (Van Bergen *et al.*, 1983).
In this paper we present new petrological and mineral chemistry data on the metamorphic xenoliths and magmatic inclusions. The petrological study carried out on the magmatic inclusions gives new information on the possible chemistry of the MA mafic magma, whereas the mineral chemistry of phases present in the metamorphic xenoliths let us to define the equilibrium temperatures and pressures which could give a contribution on the knowledge of the depth of the magmatic chamber.

Chemistry of whole rocks and magmatic inclusions

Major, trace elements and CIPW norms of representative MA volcanics and magmatic inclusions are given in Table 1. Compositional variations between whole rocks and magmatic inclusions are illustrated by means the TAS diagram (Fig. 3a). As noted by previous authors (Van Bergen *et al.*, 1983), the two groups of rocks define in this diagram a continuous linear trend ranging respectively from 48-59% SiO_2 for the magmatic inclusions, to 57-69% SiO_2 for the volcanics. They both have high alkali contents ($6\%<Na_2O+ K_2O<9\%$) with an high, and practically constant, K_2O content (5-6.5%), (Tab. 1). Moreover, among the magmatic inclusions sampled, the more basic one (AM 170, Table 1) shows major and trace elements contents very close to the theoretical MA mafic end member estimated by Van Bergen (1983), obtained solving best fit correlation lines in the SiO_2 oxide/elements diagrams in which MA volcanics and magmatic inclusions have been plotted.
The magmatic affinity for MA volcanics and inclusions is different, as underline by the Irvine-Baragar (1971) boundary line reported in the TAS diagram (Fig. 3a). The MA volcanics show a subalkaline affinity, with a trachydacitic composition, except for the more recent products which have latitic composition and fall in the alkaline field. The latitic lavas, together with the magmatic inclusions, have chemical features ($MgO>3\%$, $K_2O/Na_2O>2\%$ and $K_2O>3\%$, Table 1) typical of ultrapotassic basic rocks (Fig. 3b; Foley *et al.*, 1987). According to the K_2O-SiO_2 classification scheme of Peccerillo and Taylor (1976) for the calc-alkaline suite, (Fig. 3c) the MA volcanics belong to the shoshonitic serie and, together with the trachydacites of the Tolfa and Mt. Cimini volcanic district, represents the acidic potassic alkaline rocks of PMT (Serri *et al.*, 1993). Most of inclusions are olivine normative, whereas minor are either nepheline or quartz normative (Table 1). The volcanics are quartz normative and most of them have peraluminous character, with corundum in their norme. A peraluminous character is also shown by two of the quartz normative inclusions (Table 1).

Petrography

The Mt. Amiata host lavas

The composition of products of the first phase of MA volcanic activity is trachydacitic and lavas are here named Basal Trachydacite (BT). They are followed by more viscous lavas which have given rise to numerous Trachydacitic Domes (TD). Minor lava flows, named as Late Trachydacite (LT), and two small latitic flows, Final Latites (FL), mark the end of the volcanic activity. Petrographical data of the MA host lavas have been presented by Rodolico (1935), Mazzuoli and Pratesi (1963), Dupuy (1970), Balducci e Leoni (1981), Van Bergen *et al.* (1983). A short description of the petrographic features of these products is here reported.

Basal Trachydacite (BT): these lavas have medium-grained porphyritic textures with phenocrysts of plagioclase, sanidine, biotite, ortho- and rare clinopyroxenes. The groundmass, is generally glassy and perlitic. Apatite, zircon and ilmenite are the common accessory phases. Resorbed xenocrysts of quartz may occur.

Trachydacitic Domes (TD): abundant, large ($1<\phi<5$cm) sanidine phenocrysts is the peculiar characteristic of these products. The other phenocrysts, of smaller size, are of plagioclase, ortho- and clinopyroxene, biotite and olivine. Microlites of clinopyroxenes and, more rarely, of orthopyroxene and biotite occur in the groundmass, whose texture varies from microlitic to partly or entirely glassy. As seen for BT lavas, even in the TD samples apatite, zircon and ilmenite may occur as accessory phases.

Late Trachydacites (LT): these lavas are porphyritic for plagioclase, sanidine, ortho- and clinopyroxene, biotite crystals. The accessory phases are represented by rare crystals of apatite, zircon and magnetite. In the glassy groundmass microlites of clinopyroxene, sanidine and biotite may occur.

Final Latites (FL): they are porphyric, with phenocrysts of plagioclase, clino- and orthopyroxene, biotite, olivine and very rare quartz. In the microlitic groundmass crystals of plagioclase, sanidine, clinopyroxene and minor magnetite are present.

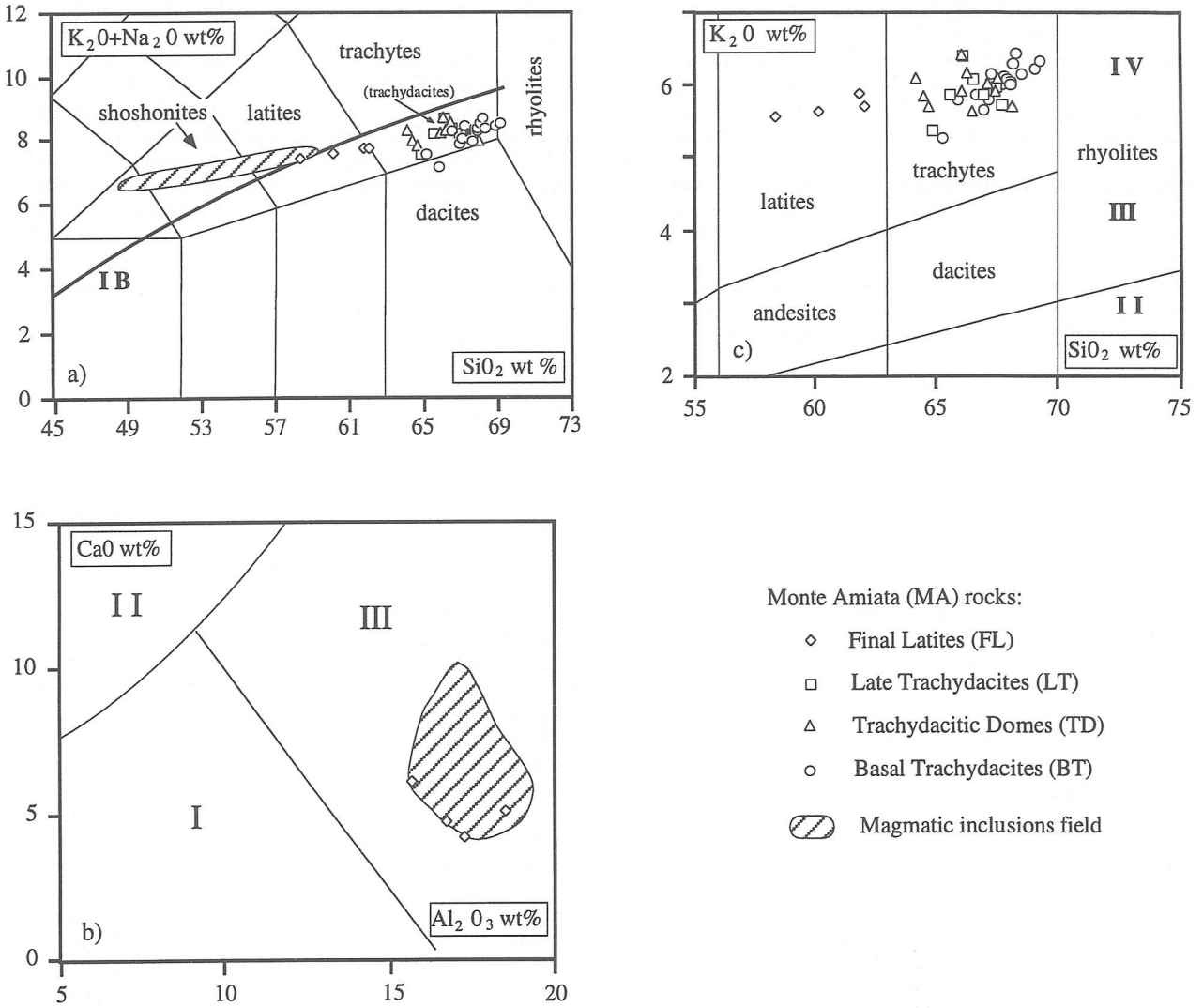

Fig. 3 - **a)** TAS classification diagram (Le Maitre et al., 1989) of analysed MA volcanics and magmatic inclusions. The IB line divides alkaline and subalkaline fields, according to Irvine and Baragar (1971). **b)** CaO vs. Al_2O_3 wt% classification diagram for ultrapotassic rocks (after Foley et al., 1987) for the MA magmatic inclusions and final latites. **c)** K_2O vs. SiO_2 wt% classification diagram (after Peccerillo and Taylor, 1976) for the MA volcanics.

MAGMATIC INCLUSIONS AND METAMORPHIC XENOLITHS

They both are relatively abundant in the MA volcanics. The magmatic inclusions are lacking in the BT lavas, whereas they frequently occur in TD and sporadically in LT and FL lavas. The metamorphic xenoliths are widespread in BT lavas, less abundant in TD and LT lavas, and relatively rare in FL lavas. Location map of the sampling sites is reported in Figure 2.

Magmatic inclusions

These inclusions, characterized by rounded shape, are relatively widespread close to the emission centres, where they show the biggest sizes (even up to 70 cm in diameter). Often the host lava shows a vesicular rim around these inclusions. Macroscopically they are very fine to fine grained and their colours vary from light to dark grey.

Microscopically they have a microcrystalline texture. In the porphyric samples, phenocrysts of ortho- and clinopyroxene, biotite and sometimes olivine are present. K-feldspar may occur and, because of its rounded shape and size (F>3 cm), they have been considered as xenocrysts (Balducci and Leoni, 1981). Cloudy aggregates of pyroxenes, plagioclase and biotite are also present. According to the amount of glass the groundmass texture ranges from variolitic to microcrystalline.

Metamorphic xenoliths

Their size, generally less than 15 cm, their angular

Tab. 1 - Representative chemical whole rock compositions and CIPW norms of MA volcanics and magmatic inclusions.

	Basal Trachydacites (BT)											Trachydacitic Domes (TD)										Late Trachydacites (LT)				
	AM 129	AM 2	AM 13	AM 132	AM 11	AM 19	AM 1	AM 133	AM 94	AM 37	AM 16	AM 104	AM 86	AM 32	AM 79	AM 82	AM 47	AM 147	AM 26	AM 29	AM 174	AM 74	AM 116	AM 65	AM 120	AM 71
SiO2	64.53	65.64	66.11	66.3	66.57	66.98	67.22	67.4	67.71	68.27	68.34	63.58	63.76	64.38	64.94	65.79	66.11	66.69	66.81	66.87	67.55	64.88	65.57	65.76	66.54	66.87
TiO2	0.58	0.51	0.5	0.6	0.52	0.54	0.52	0.5	0.49	0.48	0.48	0.57	0.58	0.57	0.6	0.55	0.57	0.47	0.52	0.5	0.51	0.53	0.58	0.53	0.52	0.51
Al2O3	16.62	16.68	15.7	15.85	15.9	16.05	15.78	15.89	16.35	15.26	15.19	16.96	16.23	16.04	16.6	16.32	15.91	16.75	15.58	15.97	16.04	17.83	16.21	16.42	15.97	15.95
Fe2O3	3.3	2.11	2.07	2.2	2.06	2.56	2.15	1.96	1.78	2.14	2.41	1.64	3.37	2.14	3.05	2.53	3.04	1.59	1.44	2.1	1.79	2.53	2.29	2.31	2.30	2.18
FeO	0.78	1.06	0.91	1.38	1.38	0.59	0.86	0.83	0.86	0.64	0.36	2.31	0.43	2	0.25	0.99	0.35	1.63	1.94	1.07	1.52	0.79	1.00	0.93	0.84	0.97
MnO	0.07	0.06	2.41	0.06	0.05	0.05	0.05	0.05	0.04	0.05	0.05	0.07	0.06	0.07	0.05	0.06	0.05	0.05	0.05	0.05	0.05	0.05	0.05	0.05	0.05	0.05
MgO	1.8	1.31	0.05	1.53	1.43	1.33	1.2	1.2	1.13	1.11	1.13	2.05	2.37	2.45	1.52	1.63	1.55	1.35	1.74	1.58	1.35	1.40	1.49	1.33	1.35	1.29
CaO	3.5	2.76	2.53	3.12	3.01	2.76	2.64	2.45	2.14	2.36	2.3	3.33	4.08	3.82	2.99	2.85	3.05	2.02	2.99	2.89	2.28	2.65	2.90	2.67	2.79	2.72
Na2O	2.27	2.41	2.13	2.16	2.26	1.96	2.29	2.23	2.23	2.2	2.15	2.08	2.17	2.1	2.27	2.15	2.19	1.97	2.19	2.21	2.21	2.24	2.25	2.29	2.20	2.40
K2O	5.18	5.77	5.9	5.6	5.73	5.93	5.93	6.22	6.06	6.14	6.25	5.74	6.03	5.63	5.77	6.08	5.55	5.98	5.97	5.82	5.64	5.78	5.99	5.75	5.86	5.63
P2O5	0.24	0.18	0.19	0.22	0.2	0.18	0.18	0.17	0.17	0.15	0.15	0.23	0.21	0.22	0.22	0.21	0.2	0.17	0.18	0.18	0.19	0.20	0.20	0.18	0.18	0.18
LOI	1.13	1.5	1.51	0.98	0.87	1.06	1.2	1.12	1.03	1.01	1.2	1.44	0.7	0.58	1.74	0.84	1.43	1.33	0.58	0.96	0.87	2.37	1.47	1.80	1.39	1.25
Q	20.70	21.19	23.28	22.86	22.38	24.57	23.37	23.24	24.99	24.43	24.92	18.65	15.68	18.02	20.68	20.98	22.86	25.43	21.64	23.14	25.69	21.52	20.72	22.25	22.89	23.15
C	1.49	1.88	1.66	1.09	0.99	1.82	1.23	1.44	2.64	0.70	1.07	1.82		0.07	1.71	1.52	1.23	3.77	0.51	1.57	2.61	3.55	1.23	2.01	1.37	1.39
or	30.61	34.10	34.86	33.09	33.86	35.04	35.04	36.75	35.81	36.28	36.93	33.92	35.63	33.27	34.10	35.93	32.80	35.34	35.28	34.39	33.33	34.15	35.40	33.98	34.63	33.27
ab	19.21	20.39	18.02	18.28	19.12	16.58	19.38	18.87	18.87	18.61	18.19	17.60	18.36	17.77	19.21	18.19	18.53	16.67	18.53	18.70	18.70	18.95	19.04	19.38	18.61	20.31
an	15.80	12.52	11.31	14.04	13.63	12.52	11.92	11.04	9.51	11.72	10.43	15.02	16.74	17.51	13.40	12.77	13.83	8.91	13.66	12.17	10.07	11.84	13.08	12.07	12.67	12.32
ne																										
di													1.72													
hy	7.34	5.44	6.50	6.23	5.97	5.35	4.97	4.80	4.50	4.58	4.60	8.01	7.63	9.14	5.83	6.47	6.04	5.68	6.74	6.11	5.69	5.71	5.85	5.48	5.45	5.34
ol																										
mt	1.87	1.48	1.39	1.68	1.62	1.45	1.40	1.30	1.23	1.28	1.26	1.89	1.73	1.96	1.50	1.63	1.54	1.53	1.62	1.48	1.57	1.53	1.53	1.50	1.45	1.47
il	1.10	0.97	0.95	1.14	0.99	1.03	0.99	0.95	0.93	0.91	0.91	1.08	1.10	1.08	1.14	1.04	1.08	0.89	0.99	0.95	0.97	1.01	1.10	1.01	0.99	0.97
ap	0.57	0.43	0.45	0.52	0.47	0.43	0.43	0.40	0.40	0.36	0.36	0.54	0.50	0.52	0.52	0.50	0.47	0.40	0.43	0.43	0.45	0.47	0.47	0.43	0.43	0.43
aq	1.13	1.50	1.51	0.98	0.87	1.06	1.20	1.12	1.03	1.01	1.20	1.44	0.70	0.58	1.74	0.84	1.43	1.33	0.58	0.96	0.87	2.37	1.47	1.80	1.39	1.25
D.I.	70.52	75.68	76.17	74.23	75.37	76.19	77.79	78.87	79.67	79.33	80.04	70.17	69.67	69.06	73.98	75.10	74.19	77.44	75.44	76.23	77.72	74.63	75.15	75.61	76.13	76.73
Nb	17	18	18	18	17	17	18	17	17	17	17	15	15	15	15	18	17	18	17	15	16	19	17	15	18	18
Zr	238	240	229	240	233	242	241	223	237	225	237	248	234	242	245	255	240	237	218	237	252	240	234	249	236	248
Y	44	44	40	40	38	41	43	43	43	40	44	40	40	40	44	38	43	43	40	41	42	41	46	44	43	43
Sr	409	388	360	374	388	399	387	407	368	382	366	418	535	497	410	420	379	418	450	391	312	390	410	391	395	377
Rb	331	368	373	357	363	377	380	378	388	385	395	350	360	350	363	367	368	378	368	363	373	350	372	358	368	370
Ce	153	153	144	148	144	144	147	152	139	143	144	156	145	151	153	137	155	145	140	147	154	156	156	149	153	152
Ba	584	551	525	560	535	578	556	672	610	587	571	554	739	666	577	603	465	589	591	575	422	584	581	557	530	511
La	87	85	80	81	80	84	83	79	78	82	83	84	81	82	85	77	86	79	79	80	83	86	92	98	85	85
Ni	14	12	9	12	14	9	11	14	10	8	9	19	21	34	12	12	12	15	18	17	13	10	11	12	10	9
V	62	49	47	57	54	48	46	46	45	43	42	67	75	79	61	56	58	47	55	54	49	49	58	49	49	49
Co	12	8	8	9	9	9	8	8	7	7	7	13	13	15	10	10	9	10	11	10	9	9	9	10	8	9

	Final Latites (FL)				Magmatic inclusions																					
	AM 184	AM 27	AM 87	AM 138	AM 170	AM 101	AM 176	AM 144	AM 103	AM 189	AM 179	AM 181	AM 100	AM 89	AM 180	AM 187	AM 143	AM 52	AM 175	AM 107	AM 140	AM 99	AM 45	AM 96	AM 85
SiO2	57.37	59.63	61.16	61.42	48.28	50.72	50.74	51.02	51.05	51.41	51.45	51.64	51.77	51.8	51.98	52.9	53.01	53.54	54.34	54.43	55.08	55.32	55.35	58.28	59.03
TiO2	0.74	0.66	0.64	0.64	0.88	0.91	0.87	0.8	0.92	0.84	0.88	0.88	0.89	0.91	0.84	0.98	0.91	0.82	0.83	0.77	0.79	0.91	0.81	0.76	0.77
Al2O3	18.48	15.70	17.20	16.70	17.25	17.39	18.51	16.24	16.81	17.47	17.14	19.05	18.43	18.22	18.89	18.69	17.84	17.99	18.73	17.76	17.55	17.66	18.51	17.63	17.24
Fe2O3	1.64	3.56	2.00	3.69	4.08	4.21	3.22	3.49	4.62	4.06	4.02	3.28	3.07	2	4.99	4.33	4.49	3.78	3.29	2.21	3.6	4.18	2.97	3.45	3.89
FeO	3.61	1.40	2.68	0.78	3.15	2.69	3.94	3.7	2.51	3.1	2.95	3.65	3.51	4.97	1.64	2.36	2.71	2.8	2.88	4.23	2.64	1.98	3.4	1.92	1.68
MnO	0.08	0.09	0.08	0.08	0.14	0.12	0.12	0.12	0.12	0.11	0.12	0.11	0.11	0.11	0.11	0.11	0.12	0.11	0.1	0.11	0.11	0.1	0.11	0.09	0.09
MgO	3.65	4.08	2.99	3.02	8.26	6.72	6.22	7.61	6.62	6.62	6.63	5.08	5.54	4.65	5.26	4.01	5.55	4.84	4.66	5.44	4.97	4.82	4.33	3.83	3.16
CaO	5.15	6.15	4.19	4.73	9.88	7.95	7.27	8.67	8.53	7.99	8.25	6.08	7.06	7.28	6.33	6.88	8.16	6.68	6.36	6.25	6.43	5.94	4.8	4.69	5.39
Na2O	1.79	1.91	1.84	1.96	0.75	1.43	1.32	1.19	1.51	1.5	1.31	1.64	1.59	2.02	1.74	1.71	1.42	1.74	1.62	1.25	1.6	1.51	1.52	1.85	1.96
K2O	5.44	5.55	5.79	5.63	5.25	5.75	5.89	5.18	5.23	5.2	5.44	6.18	5.99	5.73	5.95	5.92	4.01	6.03	5.51	5.45	5.15	6.18	5.78	5.93	5.56
P2O5	0.27	0.27	0.26	0.24	0.34	0.5	0.42	0.42	0.48	0.46	0.38	0.43	0.44	0.52	0.43	0.47	0.49	0.41	0.35	0.37	0.38	0.35	0.32	0.29	0.31
LOI	1.77	1.01	1.19	1.13	1.77	1.61	1.49	1.56	1.59	1.24	1.45	1.97	1.59	1.78	1.84	1.64	1.3	1.27	1.33	1.74	1.71	1.06	2.1	1.27	0.91
Q	8.35	9.23	13.76	13.24													3.47		2.02	3.40	4.15	2.36	6.01	7.85	9.48
C	0.93		0.91																				1.79	0.33	
or	32.15	32.80	34.21	33.27	31.02	33.98	34.80	30.61	30.90	30.73	32.15	36.52	35.40	33.86	35.16	34.98	23.70	35.63	32.56	32.20	30.43	36.52	34.15	35.04	32.85
ab	15.15	16.16	15.57	16.58	1.79	11.30	11.17	10.07	12.78	12.69	11.08	13.88	13.45	17.05	14.72	14.47	12.01	14.72	13.71	10.58	13.54	12.78	12.86	15.65	16.58
an	23.79	17.87	19.09	20.14	28.20	24.05	27.19	23.67	23.64	25.58	24.82	26.37	25.46	23.72	26.16	25.84	30.46	23.47	27.56	26.75	25.49	23.16	21.72	21.37	21.82
ne					2.47	0.44								0.02											
di		8.76		1.42	14.90	9.75	4.95	13.33	12.50	8.90	10.96	0.80	5.40	7.31	1.97	4.25	5.52	5.67	1.38	1.48	3.17	3.25			2.35
hy	13.65	10.12	11.50	10.47			2.17	5.08	2.09	6.05	5.23	5.36	3.30		6.18	11.39	17.82	10.67	16.62	19.08	16.66	15.87	16.37	14.01	11.36
ol					14.56	13.25	12.83	10.39	10.76	9.32	9.02	9.73	10.12	10.68	8.68	1.80		3.47							
mt	2.17	1.96	1.91	1.75	2.63	2.50	2.64	2.64	2.57	2.61	2.53	2.55	2.42	2.61	2.37	2.41	2.61	2.39	2.25	2.40	2.27	2.22	2.59	2.14	2.21
il	1.41	1.25	1.22	1.22	1.67	1.73	1.65	1.52	1.75	1.60	1.67	1.67	1.69	1.73	1.60	1.86	1.73	1.56	1.58	1.46	1.50	1.73	1.54	1.44	1.46
ap	0.64	0.64	0.62	0.57	0.81	1.18	0.99	0.99	1.14	1.09	0.90	1.02	1.04	1.23	1.02	1.11	1.16	0.97	0.83	0.88	0.90	0.83	0.76	0.69	0.73
aq	1.77	1.01	1.19	1.13	1.77	1.61	1.49	1.56	1.59	1.24	1.45	1.97	1.59	1.78	1.84	1.64	1.30	1.27	1.33	1.74	1.71	1.06	2.10	1.27	0.91
D.I.	55.64	58.19	63.54	63.09	32.82	45.27	45.97	40.68	43.68	43.42	43.23	50.39	48.85	50.91	49.88	49.45	39.18	50.35	48.29	46.18	48.12	51.65	53.02	58.54	58.92
Nb	14	14	15	17	12	12	12	9	11	9	12	11	12	11	9	16	14	12	14	11	9	14	12	16	12
Zr	254	247	247	244	245	236	271	234	223	236	257	236	254	249	234	271	255	270	257	255	215	275	279	271	279
Y	40	40	37	38	36	35	36	59	35	36	35	33	35	38	33	38	36	40	36	38	33	36	102	42	40
Sr	615	647	541	584	814	862	694	865	905	890	694	710	732	824	957	797	675	818	730	607	843	803	611	603	664
Rb	282	341	310	326	327	310	351	329	302	302	276	302	327	333	240	317	288	349	337	329	286	302	345	333	321
Ce	176	155	145	148	152	162	165	152	159	176	156	162	155	162	155	162	152	167	162	151	141	170	177	152	145
Ba	716	632	750	731	801	952	865	859	924	1020	837	1074	948	1024	956	998	731	848	847	680	843	837	733	737	671
La	95	87	77	82	81	81	84	116	84	97	78	89	86	82	80	93	91	93	81	84	76	89	207	86	87
Ni	30	45	30	28	79	55	27	62	57	64	50	80	45	30	58	31	36	31	27	57	98	32	37	35	23
V	109	111	86	92	190	196	173	186	204	205	159	219	177	171	204	153	137	166	170	158	224	135	132	112	113
Co	18	19	15	15	30	29	26	31	30	30	25	32	28	26	28	25	23	26	26	27	36	23	25	21	20

D.I. = Q+Or+Ab+Ne+Le (Thornton and Tuttle, 1960).
The Fe203/Fe0 ratios suggested by Middlemost (1989) have been used for norms calculation.

Tab. 2 - Index of mineral assemblages for metamorphic xenoliths.

	Sample	MA volcanic	K-feldspar	Plagioclase	Quartz	Sillimanite	Cordierite	Spinel	Biotite	Garnet	Orthopyroxene	Clinopyroxene	Graphite	Other
Assemblage "a"	AM 63	LT	X		X				X		X		X	
	AM 83	TD	X	X	X				X		X		X	
Assemblage "b"	**AM 38**	BT	X	X		X	X	X	X	X			X	corundum
	AM 66	LT	X	X		X		X	X		X			corundum
	AM 171	TD	X	X		X		X	X				X	oxides
Assemblage "c"	AM 7	BT	X	X				X	X		X		X	
	AM 18	BT	X	X				X	X		X		X	
	AM 67	LT	X	X				X	X		X			glass
	AM 88	FL	X	X*			X	X*	X		X		X	
	AM 142	FL	X	X				X	X		X	X1	X	
	AM 151	TD	X	X				X	X		X		X	

*= rare; X1= as rim of orthopyroxene. In bold are reported the samples analysed by electron micropobe.

Tab. 3 - Representative micrprobe chemical analyses (wt%) of olivine crystals (basis of 4 oxygens)

	Trachydacitic Domes (TD)		Final Latites (FL)				
	AM 84		AM 138				
	ph	ph	ph	ph	ph	ph(c)	ph (r)
SiO2	34.82	34.43	34.45	34.55	34.78	40.29	39.87
FeO	42.92	44.88	46.14	43.93	42.65	14.00	14.52
MnO	0.83	0.74	0.84	0.82	0.82	0.25	0.34
MgO	22.29	20.68	19.78	20.84	22.39	46.23	44.72
CaO	0.07	0.08	0.18	0.24	0.28	0.30	0.33
NiO	0.00	0.00	0.00	0.00	0.00	0.00	0.00
Tot.	100.93	100.81	101.39	100.38	100.92	101.07	99.78
Si	0.998	0.998	0.999	1.002	0.996	0.996	1.002
Fe	1.029	1.088	1.119	1.066	1.022	0.290	0.305
Mn	0.020	0.018	0.021	0.020	0.020	0.005	0.007
Mg	0.953	0.894	0.856	0.902	0.957	1.705	1.675
Ca	0.002	0.002	0.006	0.007	0.009	0.008	0.009
Ni	0.000	0.000	0.000	0.000	0.000	0.000	0.000
Fo %	48.08	45.10	43.32	45.82	48.35	85.48	84.59

ph=phenocryst; (c)=core; (r)=rim

shape and their usually dark colour are macroscopic useful features to distinguish them from the magmatic inclusions. Detailed petrographic descriptions of the MA metasedimentary xenoliths have been presented elsewhere (Van Bergen, 1983; Van Bergen and Barton, 1984). Van Bergen (1983) classified these xenoliths as fine-grained hornfels like rocks, representing the fragments of the contact aureole formed during the emplacement of magma in the pre-Mesozoic sediments from the tuscan crystalline basement.

Eleven metamorphic xenoliths have been studied petrographically among those sampled from sites indicated in Figure 2.

In Table 2 is reported a summary of the mineralogy of studied samples. Three distinct groups of xenoliths can be distinguished based on the mineralogical associations:

assemblage a): it consists of quartz, plagioclase, sanidine, biotite, graphite and orthopyroxene;

assemblage b): it is made of sillimanite, plagioclase, sanidine, biotite, corundum, spinel, cordierite and garnet;

assemblage c): with sanidine, plagioclase, biotite, spinel, orthopyroxene and glass.

Assemblage a and *c* show granoblastic texture, with lenticular structure made of spinel and glass, while *assemblage b* has typical porphyroblastic texture.

Mineral chemistry

Chemical analyses were performed at the University

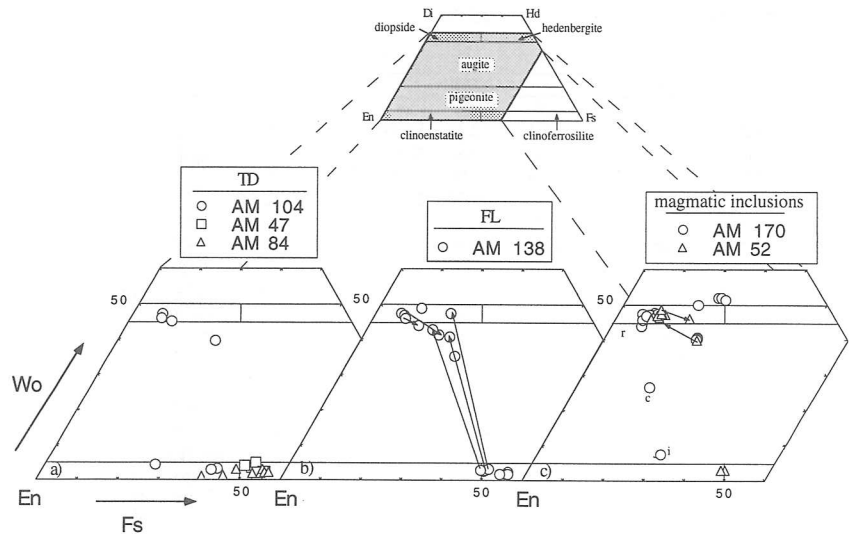

Fig. 4 - Clinopyroxene compositions projected in the Wo-En-Fs ternary system. Nomenclature after Morimoto (1989). TD=trachydacite domes; FL=final latites. In diagram c) the label c=core, i=intermediate, and r=rim are referred to the cpx 1 analyses of AM170 reported in Tab. 4 - The arrows reported on the diagrams indicate the changes in the composition going from the core to the rim of the crystal. See text for further discussion.

of Florence by means of an automated Jeol JXA 8600 electron microprobe operating with variable beam current (10 nA) and accelerating voltage (15 kV). Representative analyses of analysed phases are given in Tables 3 to 6, and in Table 8. For same samples the mineral chemistry was obtained by scanning electron microscopy (SEM-EDAX) at the University of Pisa (analytical conditions: 20Kv, 10nA). In Table 7 the average chemical composition of the analysed phases is reported. Differences between the two analytical systems were tested by analysing the same clinopyroxene phenocrysts in the samples AM138 and AM52. The differences found are within a relative analytical errors of 1% (∂x).

Host lavas and magmatic inclusions

Olivine: representative analyses of olivine crystals are reported in Table 3. The Mg-rich olivine (Fo_{85}) has been found in a FL sample in which more fayalitic olivine crystals (Fo_{48-43}) are present too. In the siliceous lavas (TD) instable olivine have a composition of Fo_{48-45}.

Pyroxenes: their compositions have been projected in the Wo-En-Fs ternary system using nomenclature after Morimoto (1989) (Fig. 4). Orthopyroxene (opx) in the TD rocks reveals the more wide variations with a relatively high Fe content, and Mg# ratios ($100Mg/(Mg+Fe^{2+})$) ranging between 44 and 73; wollastonite contents do not exceed 5% (Tab. 4). The chemical composition of opx is quite similar in both FL and magmatic inclusions (Fig. 4b, c): the Mg# ratios range between 45 and 52 and the Fe content is lower than that observed in the TD orthopyroxenes.
Clinopyroxene (cpx) in the TD is prevalent diopside and it rarely has an augitic composition (Fig. 4a); in the FL it has a diopsidic composition in the core trending towards augitic in the rim. Moreover, in the FL the small rims of cpx, surrounding the resorbed opx crystals, have augitic composition (Fig. 4b). In the magmatic inclusions cpx shows both reverse and oscillatory zoning with a composition ranging from diopside to hedenbergite to augite (Fig. 4c). In AM 52 (inclusion of FL lavas) cpx crystals with a core of augitic (En_{37}-Fs_{22}-Wo_{40}) and a rim of diopside (En_{43}-Fs_{9}-Wo_{47}) composition coexist with crystals having a diopsidic (En_{41}-Fs_{10}-Wo_{49}) core and an augitic (En_{36}-Fs_{18}-Wo_{46}) rim (Fig. 4c, Table 4). Moreover, in the more basic inclusion (AM 170, inclusion of TD lavas) cpx phenocrysts show an oscillatory zoning with composition changing abruptly from hedenbergite to diopside (i.e. cpx 2, Tab. 4); in the same xenoliths skeletal crystals having cores with sanidine, probably crystallized from trapped liquid, are present (Fig. 5b).

Feldspars: compositions of feldspars are plotted in Figure 6. The plagioclases of TD and FL generally show strong variations in An content, and variable zoning (Fig. 6a; Tab. 5). In the TD samples, the plagioclases reveal both normal (core=An_{77}, rim=An_{56}) than reverse (core=An_{54}, rim=An_{82}) zonings. Among these samples, the plagioclases of the AM47 sample show complex zoning, with the more calcic composition (An_{87-77}) present both in the core and in the rim zones of crystals (Tab. 5). The compositions of plagioclase in the FL are less anorthitic (An_{77-48}) than that present in the TD plagioclases, even if they cover the same trend described by these last one. In the magmatic inclusions the plagioclase crystals do not exhibit a pronounced chemical variation having an An_{61-54} content (Tab. 5, Fig. 6b).

Sanidine: occurs as phenocrysts in the TD, while in the magmatic inclusions and in the FL it shows rounded outlines which point to a xenocrystal origin. Sanidine composition in TD and FL shows little variation, whereas in the magmatic inclusions it shows the more sodic content (Tab. 5, Fig. 6).

Tab. 4 - Representative microprobe chemical analyses (wt%) of pyroxene (basis of 6 oxygens).

	Trachydacitic domes (TD)														
	AM 104						AM47			AM 84					
	ph(c)	ph(r)	ph	ph	ph(c)	ph(r)	ph	ph	ph	ph	ph	ph	ph	ph	ph
SiO2	51.47	54.74	50.30	51.35	52.01	50.58	50.41	50.58	50.95	52.58	51.84	50.46	50.39	50.83	50.21
TiO2	0.39	0.17	0.29	0.34	0.43	0.89	0.26	0.36	0.14	0.04	0.30	0.19	0.13	0.28	0.07
Al2O3	1.02	0.46	0.96	1.28	3.63	4.61	1.57	1.07	0.34	0.38	0.89	0.53	0.42	0.67	0.37
FeO	26.30	17.21	31.89	14.18	4.19	5.99	31.19	29.71	31.89	24.50	27.42	30.98	32.64	28.83	33.24
MnO	0.70	0.68	0.80	0.52	0.19	0.10	0.92	0.68	0.90	0.69	0.66	0.83	1.02	0.76	0.99
MgO	18.91	25.15	14.55	12.65	16.51	15.52	15.04	16.10	15.30	20.59	18.55	15.52	14.37	16.97	14.16
CaO	1.77	2.45	1.35	19.30	22.86	22.15	0.98	2.15	1.29	0.70	0.81	1.13	1.28	1.68	1.27
Na2O	0.08	0.00	0.08	0.17	0.15	0.13	0.00	0.00	0.00	0.00	0.00	0.07	0.00	0.00	0.00
K2O	0.00	0.00	0.00	0.00	0.00	0.05	0.00	0.00	0.01	0.01	0.02	0.01	0.00	0.02	0.00
Cr2O3	0.06	0.00	0.08	0.17	0.35	0.00	0.00	0.01	0.00	0.08	0.02	0.07	0.00	0.02	0.02
Tot.	100.70	100.86	100.30	99.96	100.32	100.02	100.37	100.66	100.82	99.57	100.51	99.79	100.25	100.06	100.33
Si	1.945	1.981	1.966	1.948	1.892	1.857	1.962	1.948	1.977	1.991	1.972	1.971	1.977	1.960	1.972
Ti	0.011	0.005	0.009	0.010	0.012	0.025	0.008	0.010	0.004	0.001	0.009	0.006	0.004	0.008	0.002
Al IV	0.055	0.019	0.034	0.052	0.108	0.143	0.038	0.052	0.023	0.009	0.028	0.029	0.023	0.040	0.028
Al VI	-0.010	0.001	0.010	0.006	0.048	0.056	0.034	-0.003	-0.008	0.008	0.011	-0.004	-0.003	-0.009	-0.011
Fe3+	0.046	0.008	0.011	0.034	0.037	0.050	0.000	0.034	0.023	0.000	0.000	0.026	0.019	0.034	0.033
Fe2+	0.785	0.513	1.031	0.416	0.090	0.134	1.015	0.923	1.012	0.776	0.872	0.986	1.053	0.896	1.059
Mn	0.022	0.021	0.026	0.017	0.006	0.003	0.030	0.022	0.030	0.022	0.021	0.027	0.034	0.025	0.033
Mg	1.066	1.357	0.848	0.716	0.896	0.849	0.873	0.925	0.885	1.162	1.052	0.904	0.841	0.976	0.829
Ca	0.072	0.095	0.057	0.785	0.891	0.871	0.041	0.089	0.054	0.028	0.033	0.047	0.054	0.069	0.053
Na	0.006	0.000	0.006	0.013	0.011	0.009	0.000	0.000	0.000	0.000	0.000	0.005	0.000	0.000	0.000
K	0.000	0.000	0.000	0.000	0.000	0.002	0.000	0.000	0.000	0.000	0.001	0.000	0.000	0.001	0.000
Cr	0.002	0.000	0.002	0.005	0.010	0.000	0.000	0.000	0.000	0.002	0.001	0.002	0.000	0.001	0.001
Wo	3.64	4.82	2.90	40.23	46.55	45.74	2.12	4.50	2.72	1.44	1.69	2.41	2.74	3.51	2.71
En	54.13	68.78	43.55	36.70	46.79	44.60	45.25	46.93	44.85	59.11	53.75	46.04	42.77	49.41	42.00
Fs	42.23	26.40	53.54	23.07	6.66	9.66	52.63	48.57	52.43	39.45	44.56	51.55	54.49	47.08	55.30
#Mg	57.59	72.58	45.12	63.24	90.85	86.35	46.23	50.04	46.67	59.96	54.68	47.82	44.41	52.12	43.93

	Final Latites (FL)														
	AM 138														
	ph	ph(c)	ph(r)	ph	ph(c)	ph(r)	ph(c)	ph(r)	ph	mph	ph(c)	ph(r)	ph(c)	ph(r)	mph
SiO2	50.34	51.01	51.87	50.63	51.01	50.04	52.74	51.60	50.58	49.44	51.00	51.47	52.06	50.14	51.51
TiO2	0.21	0.27	0.39	0.10	0.29	0.87	0.30	0.46	0.25	0.90	0.18	0.58	0.50	0.35	0.43
Al2O3	0.63	0.59	0.99	0.22	0.87	4.20	2.78	1.50	0.85	5.39	0.61	3.33	3.10	2.77	3.53
FeO	29.70	29.92	12.86	32.99	29.49	9.60	3.51	10.98	29.90	5.95	28.89	7.18	4.56	10.84	4.17
MnO	0.79	0.85	0.45	1.11	0.80	0.37	0.18	0.36	0.75	0.13	0.74	0.24	0.07	0.45	0.14
MgO	16.36	16.72	13.21	14.46	16.42	14.11	16.61	13.99	15.90	14.10	16.76	15.41	16.45	11.84	16.36
CaO	1.60	1.49	20.08	1.35	1.64	20.80	23.76	20.28	1.76	23.72	1.65	21.69	23.01	23.05	23.39
Na2O	0.00	0.00	0.15	0.03	0.05	0.05	0.16	0.08	0.00	0.20	0.00	0.22	0.09	0.24	0.17
K2O	0.00	0.03	0.03	0.00	0.03	0.03	0.02	0.00	0.02	0.00	0.00	0.00	0.00	0.04	0.02
Cr2O3	0.03	0.08	0.00	0.00	0.00	0.00	0.72	0.03	0.00	0.04	0.11	0.02	0.21	0.04	0.17
Tot.	99.66	100.96	100.03	100.89	100.60	100.07	100.78	99.28	100.01	99.87	99.94	100.14	100.05	99.76	99.89
Si	1.957	1.957	1.957	1.975	1.962	1.863	1.910	1.948	1.964	1.824	1.971	1.894	1.902	1.892	1.881
Ti	0.006	0.008	0.011	0.003	0.008	0.024	0.008	0.013	0.007	0.025	0.005	0.016	0.014	0.010	0.012
Al IV	0.043	0.043	0.043	0.025	0.038	0.137	0.090	0.052	0.036	0.176	0.029	0.106	0.098	0.108	0.119
Al VI	-0.014	-0.017	0.001	-0.015	0.002	0.047	0.028	0.014	0.003	0.059	-0.001	0.038	0.035	0.015	0.033
Fe3+	0.043	0.043	0.032	0.037	0.024	0.046	0.037	0.017	0.020	0.081	0.016	0.051	0.035	0.092	0.071
Fe2+	0.922	0.916	0.374	1.039	0.925	0.253	0.069	0.330	0.951	0.103	0.918	0.170	0.104	0.250	0.057
Mn	0.026	0.028	0.014	0.037	0.026	0.012	0.006	0.012	0.025	0.004	0.024	0.007	0.002	0.014	0.004
Mg	0.948	0.956	0.743	0.841	0.942	0.783	0.897	0.787	0.920	0.776	0.966	0.846	0.896	0.666	0.891
Ca	0.067	0.061	0.812	0.056	0.068	0.830	0.922	0.820	0.073	0.938	0.068	0.855	0.901	0.932	0.915
Na	0.000	0.000	0.011	0.002	0.004	0.004	0.011	0.006	0.000	0.014	0.000	0.016	0.006	0.018	0.012
K	0.000	0.001	0.001	0.000	0.001	0.001	0.001	0.000	0.001	0.000	0.000	0.000	0.000	0.002	0.001
Cr	0.001	0.002	0.000	0.000	0.000	0.000	0.021	0.001	0.000	0.001	0.003	0.001	0.006	0.001	0.005
Wo	3.37	3.10	41.40	2.86	3.45	43.40	47.89	41.97	3.73	49.43	3.47	44.50	46.52	48.03	47.34
En	47.88	48.36	37.90	42.61	48.10	40.97	46.59	40.29	46.85	40.89	49.08	44.00	46.28	34.33	46.07
Fs	48.75	48.54	20.70	54.53	48.45	15.63	5.52	17.74	49.42	9.68	47.45	11.50	7.20	17.63	6.59
#Mg	50.70	51.07	66.53	44.73	50.46	75.62	92.82	70.47	49.19	88.28	51.27	83.22	89.61	72.68	94.03

Tab. 4 (continued)

	Magmatic inclusions													
	AM170						CPX 1			CPX 2				
	ph(c)	ph(r)	ph(c)	ph(i)	ph(r)1	ph(r)2	ph(c)	ph(i)	ph(r)	ph(c)	ph(i)1	ph(i)2	ph(r)	ph
SiO2	51.74	50.17	52.06	52.67	42.37	41.63	53.98	53.37	51.38	51.32	53.40	51.56	52.91	49.66
TiO2	0.43	0.90	0.43	0.39	1.34	1.22	0.07	0.06	0.52	0.29	0.21	0.36	0.33	0.79
Al2O3	3.74	5.77	3.66	2.48	12.07	12.37	0.28	0.21	4.51	1.17	1.47	1.34	2.52	5.57
FeO	3.55	5.00	3.27	4.19	12.48	13.36	11.10	18.89	3.99	13.53	4.26	13.47	3.96	5.57
MnO	0.10	0.20	0.15	0.15	0.23	0.28	0.46	0.57	0.06	0.49	0.17	0.46	0.12	0.12
MgO	16.33	14.91	16.38	17.30	7.83	7.65	19.90	22.13	16.11	12.56	17.45	12.55	16.96	14.96
CaO	23.07	22.97	23.28	22.84	22.76	22.79	13.54	3.98	23.05	19.76	22.08	19.53	22.86	23.21
Na2O	0.15	0.24	0.18	0.12	0.21	0.23	0.11	0.10	0.10	0.16	0.10	0.13	0.15	0.22
K2O	0.00	0.00	0.00	0.00	0.05	0.05	0.00	0.00	0.00	0.04	0.00	0.03	0.00	0.00
Cr2O3	0.59	0.06	0.54	0.20	0.00	0.00	0.00	0.11	0.10	0.05	0.00	0.00	0.08	0.00
Tot.	99.70	100.22	99.95	100.34	99.34	99.58	99.44	99.42	99.82	99.37	99.14	99.43	99.89	100.10
Si	1.893	1.835	1.898	1.912	1.618	1.588	1.991	1.986	1.877	1.956	1.962	1.964	1.930	1.819
Ti	0.012	0.025	0.012	0.011	0.038	0.035	0.002	0.002	0.014	0.008	0.006	0.010	0.009	0.022
Al IV	0.107	0.165	0.102	0.088	0.382	0.412	0.009	0.014	0.123	0.044	0.038	0.036	0.070	0.181
Al VI	0.054	0.084	0.056	0.018	0.161	0.144	0.004	-0.005	0.072	0.009	0.026	0.024	0.038	0.060
Fe3+	0.023	0.047	0.020	0.051	0.163	0.218	0.009	0.019	0.026	0.031	0.008	0.002	0.023	0.093
Fe2+	0.085	0.106	0.080	0.076	0.236	0.208	0.333	0.569	0.095	0.400	0.123	0.427	0.098	0.078
Mn	0.003	0.006	0.005	0.005	0.007	0.009	0.014	0.018	0.002	0.016	0.005	0.015	0.004	0.004
Mg	0.891	0.813	0.891	0.937	0.446	0.435	1.095	1.228	0.878	0.714	0.956	0.713	0.922	0.817
Ca	0.904	0.900	0.910	0.888	0.931	0.931	0.535	0.159	0.902	0.807	0.869	0.797	0.893	0.911
Na	0.011	0.017	0.013	0.008	0.016	0.017	0.008	0.007	0.007	0.012	0.007	0.010	0.011	0.016
K	0.000	0.000	0.000	0.000	0.002	0.002	0.000	0.000	0.000	0.002	0.000	0.001	0.000	0.000
Cr	0.017	0.002	0.016	0.006	0.000	0.000	0.000	0.003	0.003	0.002	0.000	0.000	0.002	0.000
Wo	47.50	48.24	47.88	45.51	52.45	51.96	27.14	8.04	47.45	41.34	44.44	41.11	46.13	47.98
En	46.79	43.57	46.88	47.97	25.11	24.27	55.50	62.19	46.14	36.57	48.87	36.76	47.63	43.03
Fs	5.71	8.20	5.25	6.52	22.45	23.77	17.36	29.77	6.41	22.09	6.69	22.13	6.24	8.99
#Mg	91.27	88.45	91.77	92.46	65.39	67.61	76.66	68.35	90.19	64.08	88.60	62.51	90.38	91.31

	AM 52										
	ph(c)	ph(r)	ph(c)	ph(r)	ph	ph	ph(c)	ph(r)	ph	mph	mph
SiO2	52.23	48.01	51.24	49.65	49.00	50.87	48.16	48.90	50.63	49.63	49.20
TiO2	0.33	1.20	0.46	0.68	0.75	0.36	1.00	0.59	0.30	0.74	0.89
Al2O3	2.56	7.00	1.26	5.76	5.83	1.04	6.96	4.07	0.94	5.91	5.71
FeO	5.15	6.67	14.01	5.76	6.28	29.15	5.71	10.92	28.45	6.14	6.12
MnO	0.22	0.23	0.48	0.18	0.17	0.80	0.15	0.41	0.85	0.10	0.20
MgO	16.06	13.89	12.85	14.78	14.47	16.48	13.88	12.30	16.78	14.80	14.47
CaO	23.02	22.20	19.50	22.43	23.12	1.65	22.91	22.28	1.68	22.19	22.80
Na2O	0.10	0.21	0.18	0.29	0.25	0.00	0.20	0.14	0.03	0.21	0.17
K2O	0.00	0.00	0.01	0.01	0.00	0.10	0.00	0.05	0.00	0.02	0.03
Cr2O3	0.10	0.04	0.01	0.06	0.08	0.00	0.05	0.00	0.01	0.09	0.05
Tot.	99.77	99.45	100	99.6	99.95	100.45	99.02	99.66	99.67	99.83	99.64
Si	1.919	1.780	1.941	1.828	1.803	1.959	1.789	1.842	1.959	1.826	1.817
Ti	0.009	0.033	0.013	0.019	0.021	0.010	0.028	0.017	0.009	0.020	0.025
Al IV	0.081	0.220	0.059	0.172	0.197	0.041	0.211	0.158	0.041	0.174	0.183
Al VI	0.030	0.086	-0.003	0.079	0.055	0.006	0.094	0.023	0.002	0.082	0.066
Fe3+	0.037	0.081	0.050	0.075	0.116	0.020	0.075	0.114	0.023	0.064	0.080
Fe2+	0.121	0.126	0.394	0.103	0.077	0.919	0.103	0.230	0.898	0.125	0.109
Mn	0.007	0.007	0.015	0.006	0.005	0.026	0.005	0.013	0.028	0.003	0.006
Mg	0.880	0.768	0.726	0.812	0.794	0.946	0.769	0.691	0.968	0.812	0.797
Ca	0.906	0.882	0.791	0.885	0.911	0.068	0.912	0.899	0.070	0.875	0.902
Na	0.007	0.015	0.013	0.021	0.018	0.000	0.014	0.010	0.002	0.015	0.012
K	0.000	0.000	0.000	0.000	0.000	0.005	0.000	0.002	0.000	0.001	0.001
Cr	0.00	0.00	0.00	0.00	0.00	0.00	0.00	0.00	0.00	0.00	0.00
Wo	46.61	47.50	40.36	47.23	48.01	3.49	49.08	46.49	3.56	46.64	47.79
En	45.25	41.36	37.01	43.31	41.81	48.45	41.38	35.72	49.43	43.29	42.20
Fs	8.14	11.14	22.63	9.47	10.18	48.07	9.55	17.79	47.01	10.07	10.01
#Mg	87.92	85.88	64.81	88.77	91.12	50.73	88.21	75.00	51.89	86.68	87.94

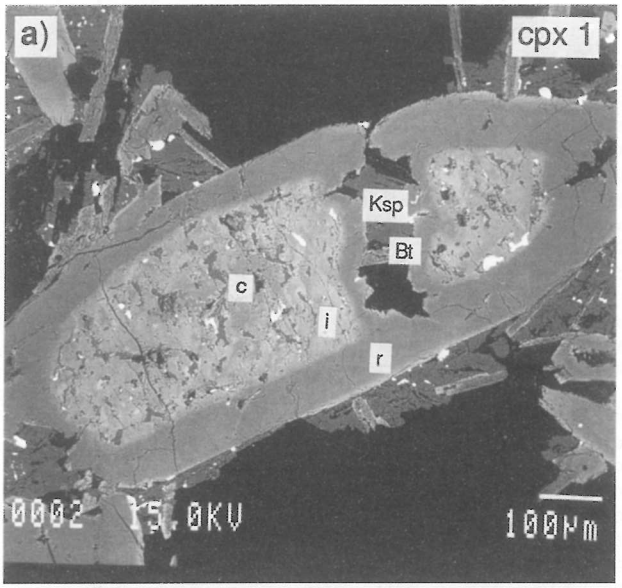

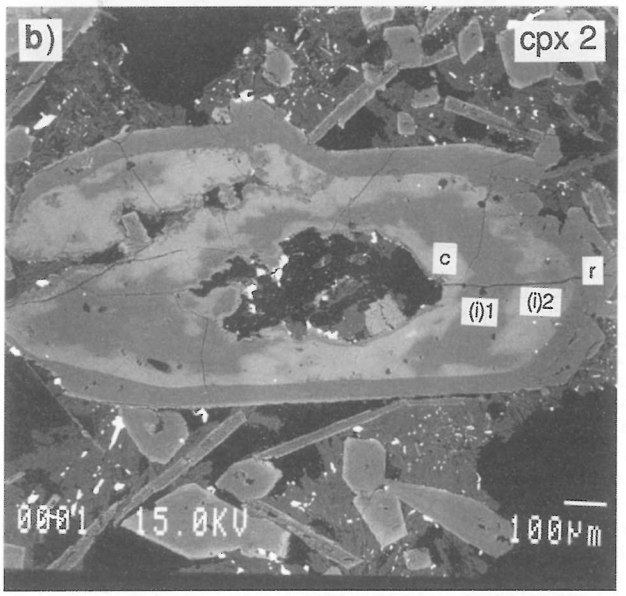

Fig. 5 - Clinopyroxenes photomicrograph of AM170 sample. In a) and in b) are reported respectively the clinopyroxenes labelled cpx 1 and cpx 2 in Table 4. c=core; i=intermediate; r=rim. In figure a) skeletal crystals of K-feldspar (Ksp) and biotite (Bt) are present. See text for further discussion.

Fe-Ti Oxides: the Fe-Ti oxides are quite exclusively represented by hematite-ilmenite solid solution with ilmenite (Ilm) content ranging from 96% to 98% (Tab. 6). Only in the magmatic inclusions spinel crystals have been found. They are characterized by a low X_{Mg} ratio $Mg/(Mg+Fe^{2+})$, variable from 0.06 to 0.1 (Tab. 6).

Metamorphic xenoliths

One sample for each mineralogical assemblage (a, b, c) described above (Tab. 2) has been analysed by electron microprobe. Representative analyses of major mineral phases are given in Table 8.

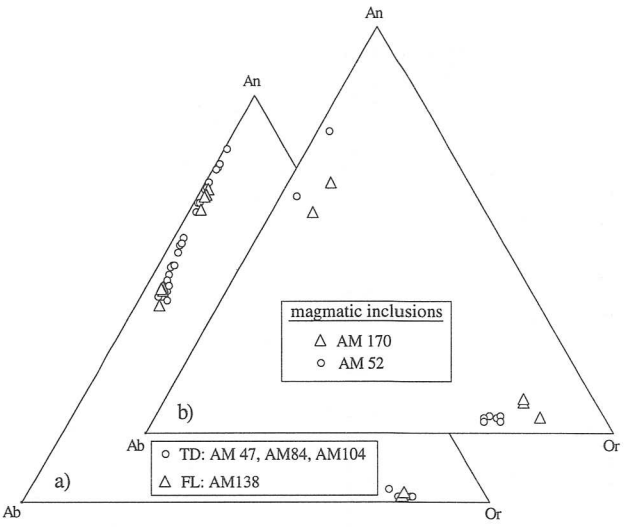

Fig. 6 - Anorthite (An)-Albite (Ab)-Orthoclase (Or) classification diagrams for the MA plagioclases.

A limited compositional range was found for the sanidine crystals belonging to *assemblages b* and *a* (Or_{76-83}).

Plagioclase (*assemblages b* and *c*) exhibits a wide chemical variation with an An content ranging from An_{49} to An_{97}.

Biotite is rather iron rich with X_{Fe} ($Fe^{2+}/(Fe^{2+}+Mg)$) ranging from 0.44 to 0.6.

Spinel is present only in the *assemblages b* and *c*. It is rich in hercynite with X_{Mg} 0.2-0.25. In the same paragenesis ilmenite crystals are present; they have a low ferric iron content, estimated from steichiometry, ranging from 0.84 to 2.2.

Fe-rich orthopyroxene (*assemblages a* and *c*) exhibits a restricted chemical composition with Mg#0.41-0.47. The composition is similar to that observed in the MA lavas (En_{40-45}, Fig. 4).

The assemblage cordierite+garnet+sillimanite±corundum is present only in the *assemblage b* (Fig. 7). Cordierite can be associated with sillimanite, spinel and plagioclase. The garnet occurs usually rounded and sometimes embayed (Fig. 7). It belongs to the pyralspite serie and it is mainly a solid solution of almandine-pyrope (Alm_{74}-Pyr_{18}-Spe_4-Gr_5) (Tab. 8). Sillimanite may occurs with a prismatic or a fibrous form. The fibrous sillimanite can be considered as a primary phase, whereas the prismatic one could be due to the replacement of andalusite.

Discussion

Previous authors (Van Bergen, 1983) observed that the straight-line correlation in the MA magmatic inclusions and the whole-rock chemistry could not be

Tab. 5 - Representative microprobe chemical analyses (wt%) of pyroxene (basis of 6 oxygens).

	Trachydacitic Domes (TD)																								
	AM 104										AM 47														
	ph(c)	ph(r)	ph	ph	ph	ph	ph	ph(c)	ph(i)	ph(r)	ph(c)	ph(r)	ph(c)	ph(r)	ph(c)	ph(r)	ph(c)	ph(i)1	ph(i)2	ph(r)	ph (c)	ph(i)	ph(r)	ph(c)	ph(r)
SiO2	56.55	55.77	54.51	46.56	55.92	54.14	53.22	65.08	63.91	64.51	49.46	55.06	55.7	47.85	65.36	65.75	56.10	48.1	46.48	50.61	48.67	56.42	54.82	48.75	52.84
Al2O3	27.19	27.59	28.20	33.48	28.69	29.71	29.93	18.79	19.31	18.99	31.99	28.15	27.72	32.87	18.52	18.57	27.62	33.16	33.51	31.13	33	27.7	28.76	31.99	29.97
FeO	0.14	0.18	0.15	0.16	0.16	0.15	0.19	0.00	0.00	0.00	0.18	0.13	0.12	0.05	0.02	0.04	0.14	0.04	0.12	0.16	0.15	0.21	0.13	0.09	0.17
CaO	10.35	10.82	11.95	17.94	10.58	11.85	12.20	0.24	0.49	0.26	15.69	11.61	11.01	16.84	0.29	0.23	10.79	16.79	17.61	14.49	16.51	10.72	11.74	16.26	13.29
Na2O	5.16	4.74	4.33	1.42	4.82	3.85	4.14	2.00	1.96	1.96	2.53	4.61	4.72	1.81	1.96	1.94	4.84	1.89	1.43	3.01	1.91	4.99	4.31	2.34	3.67
K2O	0.69	0.81	0.59	0.12	0.70	0.78	0.48	13.85	13.74	13.93	0.17	0.62	0.68	0.15	13.7	13.55	0.65	0.13	0.11	0.31	0.15	0.67	0.54	0.17	0.38
BaO	nd	nd	nd	nd	0.00	0.00	0.00	0.32	0.27	0.15	nd	nd	nd	nd	nd	nd	0.00	0.00	0.00	0.00	nd	nd	nd	nd	nd
Totale	100.08	99.91	99.73	99.68	100.87	100.48	100.16	100.28	99.68	99.80	100.02	100.18	99.95	99.57	99.85	100.08	100.14	100.11	99.26	99.71	100.39	100.71	100.30	99.60	100.32
Si	2.544	2.518	2.472	2.151	2.496	2.434	2.406	2.983	2.951	2.971	2.261	2.484	2.513	2.203	2.998	3.003	2.524	2.202	2.154	2.313	2.219	2.525	2.468	2.242	2.390
Al	1.442	1.469	1.508	1.824	1.510	1.575	1.595	1.015	1.051	1.031	1.724	1.497	1.474	1.784	1.001	1.000	1.465	1.789	1.831	1.677	1.774	1.462	1.526	1.735	1.598
Fe	0.005	0.007	0.006	0.006	0.005	0.005	0.006	0.000	0.000	0.000	0.007	0.005	0.005	0.002	0.001	0.002	0.005	0.002	0.005	0.006	0.006	0.008	0.005	0.003	0.006
Ca	0.499	0.523	0.581	0.888	0.506	0.571	0.591	0.012	0.024	0.013	0.768	0.561	0.532	0.831	0.014	0.011	0.520	0.823	0.874	0.710	0.807	0.514	0.566	0.801	0.644
Na	0.450	0.415	0.381	0.127	0.417	0.336	0.363	0.178	0.175	0.175	0.224	0.403	0.413	0.162	0.174	0.172	0.422	0.168	0.128	0.267	0.169	0.433	0.376	0.209	0.322
K	0.040	0.047	0.034	0.007	0.040	0.045	0.028	0.810	0.809	0.818	0.010	0.036	0.039	0.009	0.802	0.790	0.037	0.008	0.007	0.018	0.009	0.038	0.031	0.010	0.022
Ba	-	-	-	-	0.000	0.000	0.000	0.006	0.005	0.003	-	-	-	-	-	-	0.000	0.000	0.000	0.000	-	-	-	-	-
An	50.47	53.14	58.33	86.87	52.54	60.01	60.21	1.17	2.39	1.27	76.65	56.11	54.07	82.98	1.44	1.16	53.09	82.45	86.63	71.36	81.96	52.17	58.17	78.56	65.20
Ab	45.53	42.13	38.24	12.44	43.32	35.28	36.97	17.68	17.31	17.35	22.37	40.32	41.95	16.14	17.60	17.66	43.10	16.79	12.73	26.82	17.16	43.95	38.64	20.46	32.58
Or	4.01	4.74	3.43	0.69	4.14	4.70	2.82	81.14	80.30	81.38	0.99	3.57	3.98	0.88	80.96	81.18	3.81	0.76	0.64	1.82	0.89	3.88	3.19	0.98	2.22

	Trachydacitic Domes (TD) (continued)									Final Latites (FL)							Magmatic inclusions								
	AM 84									AM 138							AM 170					AM 52			
	ph	ph	ph(c)	ph(r)	ph(c)	ph(r)	ph(c)	ph(r)	ph	ph	ph	ph(c)	ph(i)	ph(r)	ph	ph	ph	ph	ph	ph	ph	ph	ph	ph	ph
SiO2	52.77	49.63	54.97	56.09	54.75	54.98	48.41	53.03	65.28	49.01	50.60	55.73	55.61	56.18	56.44	63.11	54.4	51.56	63.67	63.11	64	54.06	64.11	64.78	63.96
Al2O3	29.30	31.61	27.38	27.19	28.44	27.77	32.04	29.12	18.57	31.45	30.86	27.49	27.92	27.38	26.66	18.79	28.96	29.8	20.81	20.83	19.72	28.24	18.93	18.71	19.03
FeO	0.37	0.14	0.13	0.20	0.12	0.19	0.14	0.17	0.04	0.21	0.20	0.12	0.14	0.23	0.16	0.10	0.86	0.88	0.17	0.36	0.13	0.63	0.15	0.28	0.26
CaO	12.98	15.18	10.55	10.13	11.86	11.18	15.84	12.55	0.25	15.74	14.88	10.66	10.79	10.58	9.80	0.50	10.9	12.34	1.45	1.64	0.72	11.75	0.8	0.51	0.73
Na2O	3.94	2.85	4.82	5.01	4.43	4.71	2.44	4.04	2.06	2.44	2.91	4.89	4.92	4.91	5.21	1.89	4.1	3.25	1.67	1.61	1.55	4.27	2.49	2.92	2.59
K2O	0.40	0.21	0.65	0.77	0.50	0.67	0.18	0.51	13.26	0.33	0.44	0.75	0.69	0.74	0.90	13.51	1.6	1.63	12.82	12.77	14.51	0.64	12.62	12.06	12.59
BaO	nd	nd	nd	nd	nd	nd	nd	nd	0.30	0.00	nd	0.00	0.00	0.00	0.00	1.12	nd	nd	nd	nd	nd	nd	nd	nd	nd
Totale	99.76	99.62	98.50	99.39	100.10	99.50	99.05	99.42	99.76	99.18	99.89	99.64	100.07	100.02	99.17	99.02	100.82	99.46	100.59	100.32	100.63	99.59	99.1	99.26	99.16
Si	2.403	2.276	2.515	2.540	2.472	2.496	2.238	2.419	2.997	2.263	2.313	2.522	2.507	2.531	2.561	2.953	2.450	2.368	2.899	2.886	2.933	2.461	2.962	2.979	2.956
Al	1.573	1.709	1.477	1.452	1.514	1.486	1.746	1.566	1.005	1.712	1.663	1.466	1.484	1.455	1.426	1.037	1.537	1.613	1.117	1.123	1.066	1.516	1.031	1.014	1.037
Fe	0.014	0.005	0.005	0.008	0.005	0.007	0.005	0.006	0.002	0.008	0.008	0.005	0.005	0.009	0.006	0.004	0.029	0.030	0.006	0.012	0.004	0.024	0.006	0.011	0.010
Ca	0.633	0.746	0.517	0.492	0.574	0.544	0.785	0.613	0.012	0.779	0.729	0.517	0.521	0.511	0.477	0.025	0.526	0.607	0.071	0.080	0.035	0.573	0.040	0.025	0.036
Na	0.348	0.253	0.428	0.440	0.388	0.415	0.219	0.357	0.183	0.218	0.258	0.429	0.430	0.429	0.458	0.171	0.358	0.289	0.147	0.143	0.138	0.377	0.223	0.260	0.232
K	0.023	0.012	0.038	0.044	0.029	0.039	0.011	0.030	0.777	0.019	0.026	0.043	0.040	0.043	0.052	0.807	0.092	0.095	0.745	0.745	0.848	0.037	0.744	0.708	0.742
Ba	-	-	-	-	-	-	-	-	0.005	0.000	-	0.000	0.000	0.000	0.000	0.021	-	-	-	-	-	-	-	-	-
An	63.05	73.73	52.63	50.37	57.93	54.53	77.38	61.31	1.26	76.60	71.99	52.25	52.60	52.00	48.28	2.45	53.90	61.20	7.35	8.30	3.46	58.06	3.93	2.53	3.58
Ab	34.63	25.05	43.51	45.08	39.16	41.57	21.57	35.72	18.76	21.49	25.48	43.37	43.40	43.67	46.44	16.75	36.69	29.17	15.31	14.75	13.48	38.18	22.16	26.22	22.97
Or	2.31	1.21	3.86	4.56	2.91	3.89	1.05	2.97	79.99	1.91	2.53	4.38	4.00	4.33	5.28	80.80	9.42	9.63	77.34	76.95	83.05	3.77	73.90	71.25	73.46

ph=phenocryst; (c)=core; (r)=rim; mph=microphenocryst; nd=not determined

explained by any classic differentiation mechanism and a magma mixing process had to be invoked. Following this Author, a mixing process occurred between a basic and an acid end member. The composition of the mafic end member magma, estimated solving best-fit correlation lines in SiO_2-oxide/elements, has chemical characteristic similar to potassic alkaline magma of PMR. The acid end member magma is assimilated to the Basal Trachydacite (BT) lavas, which seems to be the product of a partial melting process of tuscan metapelitic rocks (Giraud *et al.*, 1986). At present the MA geochemical available data are unable to define an accurate petrogenetic model.

Regarding the MA volcanics and magmatic inclusions we use the pyroxene chemistry to infer information on the physical conditions of magma formation from which it is crystallized. The chemical variations observed in the MA clinopyroxene has been used to estimate the intensive parameters of crystallization. In Figure 8a the Al_{tot} vs Al^{VI} contents are reported. A positive correlation for FL, TD and magmatic inclusions has been observed and according to Thompson (1974) it can be explained with a change in P conditions. Moreover, an increase of Al^{IV}, as that observed in the analysed clinopyroxenes (Fig. 8b) could be due to a rise in the T, as experimentally demonstrated by Kushiro (1960) and Thompson (1974).

The positive correlation observed in Figure 8b between Al^{IV} and Al_{tot} could be due to changes in $f(O_2)$ of magma conditions, as suggested by Vieten (1980). Infact, an increase in $f(O_2)$ would determinate an increase of Fe^{3+} in the magma and a consequent increase of Fe^{3+}/Fe^{2+} in the clinopyroxenes. According to the equation $Ca^{2+}+(Mg,Fe)^{2+}+2Si^{4+}= Ca^{2+}+Fe^{3+}+Al^{3+}+Si^{4+}$, a higher content of Fe^{3+} in these crystals may force a larger amount of Al^{3+} to enter in the tetrahedral sites (Al^{IV}). According to Vieten (1980), an increase in the $f(O_2)$ also favours the entrance of Ti in the clinopyroxene structure. However, the MA clinopyroxenes do not show a positive correlation of Fe^{3+}/Fe^{2+} with Ti (Fig. 8c), so that we can exclude that $f(O_2)$ has played an important role in the chemical variations observed in the MA clinopyroxenes. We can consider the Al variations of these crystals as due mainly to changes in P and T conditions.

An interesting case is showed by the compositional variations observed in clinopyroxenes of the sample AM170, which represents the magmatic xenolith having the most basic chemical composition (Tab. 1). In the TiO_2 and FeO_{tot} vs Mg# diagrams (Fig. 8d, e) are reported the chemical data referred to two clinopyroxenes, labelled cpx 1 and cpx 2 in Table 4. The microphotos of these clinopyroxenes are reported in Figure 5: Figure 5a is referred to cpx 1, which is an example of resorbed clinopyroxene; whereas Figure 5b shows the cpx 2. In the cpx 1 the inner part is made of dark ("c" in Fig. 5a) and light ("i" in Fig. 5a) domains, which are different in chemical composition (Fig. 8d, c). The clinopyroxene cpx 2 is a well example of reverse zoning, having a rim more primitive ($Mg\#_{90}$) than core ($Mg\#_{77}$) (Fig. 8d, e). In this clinopyroxene the reverse parts are respectively near the core ($i_{(1)}$) and in the outer rim (r). According to the Mg# and FeO_{tot} contents, it seems that a mixing process with a magma having higher Mg# and lower FeO_{tot} content could have generated these reverse zonings. This magma is supposed to be hotter, as testified by the higher Al^{IV} content of the rim respect to the core.

Having the magmatic inclusion AM 170 a chemical composition very close to the theoretical one estimated by Van Bergen (1983), it can be considered as the MA mafic end member. However, the variations observed in the chemical composition of the clinopyroxenes present in this sample do not permit to consider this sample as a "true" end-member. It seems more likely that AM 170 is itself a hybrid sample derived from a mixing process involving a basic magma,

Tab. 6 - Representative composition of ilmenites and spineis. Iron recalculated after Stormer (1983).

	Ilmenites							Spinel			
	TD				FL			Magmatic inclusion			
Sample	AM 47		AM 84		AM 138			AM 170			
SiO2	0.06	0.06	0.00	0.04	0.01	0.04	SiO2	0.16	0.27	0.42	0.27
TiO2	50.96	51.71	50.70	51.48	51.43	51.94	TiO2	3.97	3.43	1.07	7.06
Al2O3	0.05	0.04	0.12	0.03	0.05	0.12	Al2O3	10.04	16.27	6.92	10.97
FeO tot	45.23	45.81	46.13	45.61	44.49	45.06	FeO tot	76.4	68.11	80	72.4
MnO	0.79	0.08	0.62	0.82	0.74	0.76	MnO	1.16	2.95	2.88	1.53
MgO	1.84	1.65	1.14	1.61	2.28	2.34	MgO	0.85	1.51	0.85	0.83
CaO	0.02	0.04	0.03	0.00	0.04	0.03	CaO	0.19	0.21	0.04	0.21
Cr2O3	0.07	0.07	0.00	0.07	0.00	0.14	Tot.	92.77	92.75	92.18	93.27
Tot.	99.02	99.46	98.74	99.66	99.04	100.43					
Fe2O3 r.	3.82	2.57	3.60	3.30	3.44	3.65	Fe2O3 r.	58.12	50.27	65.52	52.93
FeO r.	41.79	43.49	42.89	42.64	41.39	41.77	FeO r.	24.09	22.87	21.03	24.76
Tot. r.	99.40	99.72	99.10	99.99	99.38	100.79	Tot. r.	98.58	97.78	98.73	98.56
Ilm%	96.39	97.58	96.58	96.90	96.77	96.62	Mg/(Mg+Fe++)	0.059	0.105	0.067	0.056

Tab. 7 - SEM analyses (see text for discussion).

Table 7 - SEM analyses (see text for discussion)

	Basal trachydacites (BT)				Late trachydacites (LT)						Final Latites (FL)			
	AM1				AM74						AM138			
	opx				opx				cpx		cpx			
n	5		5		4		4		1	1	2		2	
	ph(c)		ph(r)		ph(c)		ph(r)		ph(c)	ph(r)	ph(c)		ph(r)	
SiO2	50.50	0.22	50.66	0.13	50.75	0.25	50.87	0.28	51.20	48.85	50.86	0.91	49.95	0.11
TiO2	0.13	0.12	0.17	0.02	0.05	0.10	0.15	0.11	0.54	1.08	0.28	0.39	0.52	0.02
Al2O3	0.64	0.22	0.52	0.09	0.70	0.23	0.56	0.16	3.37	5.24	4.12	0.55	4.38	0.51
FeO	31.22	0.47	31.13	0.21	30.17	0.86	30.57	0.49	7.19	13.36	5.17	1.16	7.44	0.16
MnO	0.74	0.13	0.64	0.10	0.67	0.09	0.65	0.12	0.00	0.25	0.00	0.00	0.00	0.00
MgO	15.42	0.22	15.63	0.16	16.26	0.78	15.94	0.21	15.29	11.34	16.39	0.59	15.70	0.06
CaO	1.32	0.14	1.25	0.11	1.30	0.13	1.23	0.04	22.23	19.85	22.60	0.64	21.44	0.71
Na2O	0.00	0.00	0.00	0.00	0.00	0.00	0.00	0.00	0.00	0.00	0.47	0.03	0.55	0.06
Tot.	99.91	0.06	99.89	0.06	99.90	0.05	99.96	0.02	99.82	99.97	99.88	0.01	99.96	0.01
En	45.51	0.64	45.99	0.47	47.65	1.91	46.93	0.73	43.32	34.26	46.12	1.13	44.51	0.62
Fs	51.69	0.66	51.38	0.30	49.60	1.78	50.47	0.70	11.43	22.64	8.17	1.92	11.82	0.38
Wo	2.80	0.31	2.64	0.23	2.74	0.27	2.60	0.08	45.26	43.10	45.71	0.79	43.66	1.00

	Magmatic inclusions													
	AM52				AM75						AM80			
	cpx				cpx						cpx			
n	5		4		4		4		6		4		4	
	ph		mph		ph(c)		ph(r)		mph		ph(c)		ph(r)	
SiO2	48.54	0.92	48.90	0.69	50.85	0.56	51.35	0.68	50.43	2.75	51.42	0.71	51.19	0.31
TiO2	0.78	0.38	0.65	0.09	0.53	0.15	0.46	0.17	0.60	0.41	0.12	0.23	0.05	0.10
Al2O3	6.36	1.86	6.08	0.90	4.73	1.51	3.12	0.74	4.03	2.98	1.18	1.43	0.00	0.00
FeO	8.46	2.75	6.89	0.24	4.91	1.03	4.72	0.95	9.12	5.97	10.21	5.60	14.66	1.07
MnO														
MgO	13.69	1.40	15.03	0.31	15.83	1.14	16.64	0.77	14.11	4.80	15.43	2.23	13.79	0.43
CaO	22.02	0.11	22.43	0.28	22.96	1.23	23.42	0.43	21.54	2.17	21.55	1.87	20.20	0.53
Na2O	0.13	0.13	0.00	0.00	0.13	0.09	0.26	0.01	0.18	0.11	0.00	0.00	0.00	0.00
Tot.	99.97	0.05	99.97	0.01	99.94	0.04	99.97	0.01	99.97	0.03	99.90	0.06	99.88	0.12
En	46.21	0.76	46.03	0.51	47.02	1.09	46.61	1.32	44.57	2.09	42.25	3.34	39.73	0.91
Fs	39.97	4.16	42.93	0.51	45.07	1.58	46.06	1.62	39.91	11.29	42.05	5.55	37.76	1.09
Wo	13.82	4.41	11.04	0.46	7.90	2.02	7.33	1.48	15.52	11.70	15.70	8.74	22.51	1.71

	Basal trachydacites (BT)						Late trachydacites (LT)					
	AM1						AM74					
	pl				kfd		pl				kfd	
n	3		4		5		5		4	4	5	
	ph(c)		ph(r)		ph(c)		ph(r)		ph(c)	ph(r)	ph(c)	
SiO2	53.34	3.10	55.58	0.55	64.27	0.09	64.06	0.11	55.88	0.31	55.95	1.18	64.20	0.18
Al2O3	30.02	2.13	28.33	0.42	19.08	0.18	19.14	0.09	28.19	0.14	28.10	0.76	19.19	0.15
CaO	12.15	2.27	10.32	0.33	0.55	0.02	0.61	0.08	10.22	0.24	10.19	0.96	0.57	0.07
Na2O	4.01	1.06	5.06	0.15	2.21	0.04	2.29	0.05	5.05	0.10	5.07	0.42	2.29	0.07
K2O	0.44	0.23	0.69	0.06	13.83	0.18	13.80	0.12	0.64	0.02	0.67	0.16	13.66	0.09
Tot.	99.96	0.04	99.98	0.01	99.94	0.04	99.90	0.05	99.98	0.00	99.97	0.01	99.91	0.06
An	60.92	11.07	50.86	1.58	2.63	0.14	2.88	0.36	50.79	0.94	50.51	4.64	2.72	0.32
Ab	36.43	9.722	45.09	1.33	19.04	0.39	19.56	0.31	45.43	1.01	45.54	3.88	19.75	0.50
Or	2.65	1.373	4.05	0.35	78.33	0.45	77.56	0.61	3.77	0.13	3.94	0.94	77.52	0.65

	Final Latites (FL)						Magmatic inclusions					
	AM138						AM80					
	pl				kfd		pl				kfd	
n	5		5		3		5		7	4	4	
	ph(c)		ph(r)		ph(c)		ph(c)		ph(r)	mph	mph	
SiO2	54.80	1.54	53.50	3.05	64.85	1.56	53.47	3.23	55.78	3.38	49.42	1.58	55.52	0.14
Al2O3	28.96	1.18	30.73	3.48	18.80	0.93	30.14	2.34	28.08	3.33	27.98	1.71	19.86	0.20
CaO	11.02	1.18	11.46	2.17	0.92	0.32	11.38	2.40	9.18	3.60	13.09	2.30	1.31	0.26
Na2O	4.63	0.66	3.78	1.60	2.41	0.04	4.40	1.27	4.56	0.89	6.82	0.58	3.74	0.30
K2O	0.56	0.18	0.50	0.22	12.70	1.32	0.59	0.24	2.37	4.43	2.67	1.03	19.54	0.73
Tot.	99.97	0.01	99.97	0.00	99.95	0.02	99.98	0.01	99.98	0.00	99.98	0.01	99.97	0.00
An	54.96	6.53	61.55	13.34	4.60	1.90	56.85	12.63	45.38	17.80	45.57	3.99	4.18	0.85
Ab	41.72	5.59	35.31	12.30	21.42	1.20	39.64	11.24	40.77	8.06	43.43	5.03	21.61	1.81
Or	3.33	1.01	3.14	1.18	73.98	3.07	3.51	1.40	13.85	25.77	11.00	3.74	74.21	2.46

Tab. 8 - Representative chemical analyses (wt%) of mineral phases present in the metamorphic xenoliths.

	AM 38									AM83		
	plagioclase						k-feldspar			k-feldspar		
			reaction rim			g. r.						
SiO2	55.02	49.77	55.67	56.75	56.05	55.94	64.4	64.42	64.82	65.35	64.98	64.64
Al2O3	28.4	31.18	28.01	27.28	28.2	28.33	19.15	19.15	18.43	19.58	19.31	19.27
Fe2O3	0.13	0.07	0.11	0.2	0.02	0.19	0.01	0.13	0.04	0	0	0
CaO	11.32	14.7	10.41	10.12	9.62	9.83	0.18	0.22	0.15	0.28	0.38	0.39
Na2O	4.85	3	5.29	5.29	5.34	5.11	1.89	2.08	2.59	2	2.06	2.1
K2O	0.59	0.27	0.69	0.69	0.79	0.78	14.33	14.02	12.93	14.01	14.05	13.84
Ba0	n.d	n.d	n.d	n.d	n.d	n.d	0.45	0.43	0.4	n.d	n.d	n.d
Tot.	100.31	98.99	100.18	100.33	100.02	100.18	100.41	100.45	99.36	101.22	100.78	100.24
	(basis of 8 oxygens)									(basis of 8 oxygens)		
Si	2.478	2.294	2.506	2.545	2.519	2.512	2.961	2.958	2.991	2.962	2.962	2.961
Al	1.508	1.694	1.486	1.442	1.494	1.500	1.038	1.037	1.003	1.046	1.038	1.041
Fe	0.004	0.002	0.004	0.007	0.001	0.006	0.000	0.004	0.001	0.000	0.000	0.000
Ca	0.546	0.726	0.502	0.486	0.463	0.473	0.009	0.011	0.007	0.014	0.019	0.019
Na	0.424	0.268	0.462	0.460	0.465	0.445	0.168	0.185	0.232	0.176	0.182	0.187
K	0.034	0.016	0.040	0.039	0.045	0.045	0.840	0.821	0.761	0.810	0.817	0.809
Ba	-	-	-	-	-	-	0.008	0.008	0.007	-	-	-
An	54.43	71.88	50.04	49.33	47.57	49.14	0.86	1.06	0.74	1.36	1.82	1.89
Ab	42.20	26.55	46.01	46.66	47.78	46.22	16.42	18.07	23.00	17.59	17.89	18.39
Or	3.38	1.57	3.95	4.00	4.65	4.64	82.71	80.88	76.26	81.054	80.29	79.73

	AM67					AM83				AM67	
	plagioclase					orthopyroxene				orthopyroxene	
SiO2	47.38	44.07	56.10	55.62	SiO2	50.7	50.39	50.45	50.07	50.62	50.53
Al2O3	33.74	35.35	27.62	27.67	TiO2	0.12	0.14	0.15	0.14	0.21	0.13
Fe2O3	0.10	0.17	0.04	0.19	Al2O3	0.35	0.53	0.53	0.59	0.37	0.49
CaO	17.56	19.82	10.90	11.09	FeO	32.08	32.28	32.25	32.63	33.70	33.35
Na2O	1.45	0.33	4.97	4.83	MnO	1.33	1.53	1.16	1.74	0.98	1.17
K2O	0.09	0.02	0.61	0.57	MgO	15.19	14.61	15.07	14.34	13.36	13.49
Ba0	n.d	n.d	n.d	n.d	CaO	1.25	0.9	0.78	0.65	1.21	1.19
Tot.	100.32	99.76	100.24	99.97	K2O	0.00	0.00	0.00	0.00	0.02	0.02
					Tot.	101.02	100.38	100.39	100.16	100.47	100.41
	(basis of 8 oxygens)					(basis of 6 oxygens)					
					Si	1.966	1.973	1.970	1.969	1.995	1.991
					Ti	0.003	0.004	0.004	0.004	0.006	0.004
Si	2.17	2.05	2.52	2.51	Al IV	0.034	0.027	0.030	0.031	0.005	0.009
Al	1.82	1.93	1.46	1.47	Al VI	-0.018	-0.003	-0.006	-0.004	0.013	0.013
Fe	0.00	0.01	0.00	0.01	Fe3+	0.045	0.021	0.027	0.026	0.000	0.000
Ca	0.86	0.99	0.53	0.54	Fe2+	0.996	1.036	1.026	1.047	1.131	1.111
Na	0.13	0.03	0.43	0.42	Mn	0.044	0.051	0.038	0.058	0.033	0.039
K	0.01	0.00	0.03	0.03	Mg	0.878	0.853	0.877	0.841	0.785	0.792
Ba	-	-	-	-	Ca	0.052	0.038	0.033	0.027	0.051	0.050
					K	0.000	0.000	0.000	0.000	0.001	0.001
An	86.54	96.96	52.86	54.07	Wo	2.64	1.94	1.66	1.41	2.62	2.59
Ab	12.93	2.92	43.62	42.62	En	44.57	43.79	44.69	43.31	40.32	40.82
Or	0.53	0.12	3.52	3.31	Fs	52.79	54.27	53.65	55.28	57.05	56.60
					Mg#	46.8	45	46	44.5	41	41.6

Tab. 8 (continued)

ILMENITES

	AM38	AM67	
SiO2	0.00	0.03	0.09
TiO2	51.94	51.66	51.46
Al2O3	0.08	0.17	0.12
FeO	44.74	44.27	44.86
MnO	0.79	0.97	0.84
MgO	1.07	1.64	1.46
CaO	0.01	0.03	0.04
Cr2O3	0.15	0.07	0.04
Tot.	98.78	98.84	98.91
(recalculated after Stormer, 1983)			
Fe2O3 r.	0.84	1.92	2.20
FeO r.	43.99	42.55	42.88
Tot. r.	98.86	99.03	99.13
Ilm %	99.20	98.19	97.91
FeO mol%	48.30	47.35	47.57
Fe2O3 mol%	0.41	0.96	1.10
TiO2 mol%	51.29	51.70	51.33

SPINELS

	AM38				AM67		
SiO2	0.00	0.00	0.00	0.02	0.00	0.00	0.05
TiO2	0.21	0.19	0.24	0.24	0.29	0.31	0.26
Al2O3	60.25	58.90	59.24	58.39	57.25	57.25	57.31
FeO	34.31	35.59	35.60	34.52	34.96	35.84	35.47
MnO	0.35	0.16	0.29	0.24	0.41	0.33	0.38
MgO	5.60	4.78	5.02	5.91	5.29	5.62	5.50
CaO	0.00	0.05	0.05	0.00	0.00	0.01	0.08
Cr2O3	0.06	-	-	0.02	0.13	-	-
Tot.	100.78	99.67	100.44	99.34	98.33	99.36	99.05
(basis on 32 oxygens)							
Fe2O3 r.	1.69	2.26	2.51	3.31	3.52	4.72	4.31
FeO r.	32.79	33.56	33.34	31.54	31.79	31.59	31.59
Tot. r.	100.95	99.90	100.69	99.67	98.68	99.83	99.48
Cr/(Cr+Al)	0.0007	-	-	0.0002	0.0015	-	-
Mg/(Mg+Fe++)	0.23	0.20	0.21	0.25	0.23	0.24	0.24

BIOTITES

	AM 38		AM 67	
SiO2	34.70	36.35	37.33	37.08
TiO2	6.25	5.82	5.74	5.86
Al2O3	15.12	14.09	13.16	13.71
FeO	23.14	17.51	19.39	18.94
MnO	0.15	0.14	0.18	0.13
MgO	8.42	12.17	11.09	10.92
CaO	0.04	0.00	0.00	0.09
Na2O	0.35	0.36	0.32	0.31
K2O	9.07	9.78	9.36	8.86
H2O+	n.d	n.d	n.d	n.d
F	1.20	2.04	1.68	1.60
Cl	0.04	0.00	0.06	0.06
Tot.	98.48	98.26	98.31	97.56
(basis on 24 anyons, according Papike 1988)				
Si	5.243	5.365	5.535	5.512
Al IV	2.757	2.635	2.465	2.488
AlVI	-0.065	-0.184	-0.165	-0.086
Ti	0.710	0.646	0.640	0.655
Fe3+	0.000	0.000	0.000	0.000
Fe2+	2.923	2.160	2.403	2.354
Mn	0.019	0.017	0.023	0.016
Mg	1.895	2.676	2.450	2.418
Ca	0.006	0.000	0.000	0.014
Na	0.102	0.103	0.092	0.089
K	1.748	1.841	1.770	1.680
OH-	n.d	n.d	n.d	n.d
F	0.573	0.952	0.787	0.752
Cl	0.000	0.000	0.000	0.000
XFe	0.606	0.446	0.495	0.493

GARNET - AM 38

SiO2	37.36	38.14	37.18	38.12	37.93	38.19
TiO2	0.03		0.05	0.02	0.04	
Al2O3	22.08	21.99	21.51	22.01	21.17	21.4
Fe2O3						
FeO	32.80	32.96	33.32	33.03	33.74	33.82
MnO	2.14	1.32	2.12	1.32	2.35	2.25
MgO	4.77	4.70	4.54	4.70	4.61	4.54
CaO	1.34	1.40	1.33	1.40	1.34	1.29
Na2O						
K2O						0.02
Cr203	0.04	0.02	0.03	0.02	0.08	0.07
(basis on 12 oxygens)						
Si	2.957	3.004	2.968	3.001	2.996	3.003
Al	0.043	0.000	0.032	0.000	0.004	0.000
Al	2.016	2.041	1.991	2.042	1.966	1.983
Cr	0.003	0.001	0.002	0.001	0.005	0.004
Fe 3+	0.000	0.000	0.000	0.000	0.000	0.000
Ti	0.002	0.000	0.003	0.001	0.002	0.000
Mg	0.562	0.551	0.540	0.551	0.542	0.532
Fe 2+	2.170	2.170	2.223	2.174	2.228	2.223
Mn	0.143	0.088	0.143	0.088	0.157	0.150
Ca	0.114	0.118	0.114	0.118	0.113	0.109
piropo	18.81	18.84	17.87	18.81	17.84	17.65
almandino	72.59	74.12	73.62	74.16	73.27	73.78
spessartina	4.80	3.01	4.74	3.00	5.17	4.97
grossularia	6.27	4.00	7.77	3.97	3.02	3.29
andradite	0.11	0.00	0.44	0.03	0.52	0.00
uvarovite	0.16	0.03	0.28	0.03	1.09	0.31

CORDIERITE - AM 38

	inside andalusite			near garnet	reaction rim
SiO2	48.59	49.41	48.74	49.23	48.76
TiO2	0.02		0.05		0.04
Al2O3	33.48	32.74	33.99	34.07	33.88
Fe2O3					
FeO	8.63	9.52	9.56	9.58	9.9
MnO	0.13	0.16	0.22	0.18	0.19
MgO	7.69	7.87	7.55	7.57	7.62
CaO	0.05	0.02	0.03	0.05	0.02
Na2O	0.06	0.1	0.14		
K2O	0.31	0.25	0.18	0.12	0.13
Cr203	0.02		0.02	0.02	
Tot.	98.98	100.07	100.48	100.82	100.54
(basis on 18 oxygens; according to Papike, 1987)					
Si	4.984	5.031	4.946	4.971	4.949
Al	4.046	3.928	4.065	4.054	4.052
Mg	1.175	1.194	1.141	1.139	1.152
Fe	0.740	0.810	0.811	0.809	0.840
Mn	0.011	0.014	0.019	0.015	0.016
Na	0.012	0.020	0.028	0.000	0.000
K	0.041	0.032	0.023	0.015	0.017
Fe+Mn / Fe+Mn+Mg	0.39	0.41	0.42	0.42	0.43

n.d.= not determined; g.r.=garnet rim; Mg#=100Mg/(Mg+Fe2+); XFe=Fe2+/(Fe2++Mg)

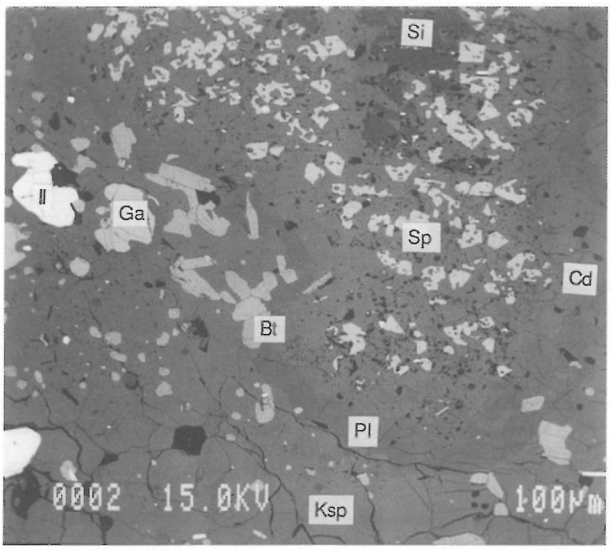

Fig. 7 - Photomicrograph of AM38 metamorphic xenolith. In the photo is well evident the coron made of the intergrowth of cordierite (Cd) and spinel (Sp) around the sillimanite (Si), which is rimmed by plagioclase (Pl) and k-feldspar (Ksp). Garnet (Ga), ilmenite (Il) and biotite (Bt) crystals are also present.

presence of orthopyroxene and sillimanite in these xenoliths testifies a high grade thermometamorphic event. During this event, temperature can reached such high values that partial melting could occur. The "c" assemblage could be a witness of these extreme thermometamorphic conditions.

The occurrence of cordierite and spinel in the "b" mineralogical assemblage (see sample AM 38, Table 8) make possible to estimate P and T conditions of the metamorphic paragenesis formation.

The T value has been estimated by means the Vielzeuf (1983) geothermometer which uses the equilibrium cordierite (Cd)-spinel (Sp). The $\ln Kd_{Sp\text{-}Cd}$ value, obtained using data reported in Table 8, yields a T value of 800°C; a similar value has been obtained from Vielzeuf (1983) on MA volcanics using the Kd values given by Van Bergen (in Kars *et al.*, 1980).

The AM 38 metamorphic xenolith is characterized by a particular texture in which sillimanite (Si) crystals are rimmed by an intergrowth of spinel (Sp)-cordierite (Cd), and commonly this rim is in turn surrounded by a corona of plagioclase (Pl) (Fig. 7). Moreover, in the same sample crystals of garnet (Ga) and corundum (C) are present. The coexistence of the five phases Cd-Sp-Ga-C-Si provides an invariant assemblage for a fixed Fe/Mg ratio in any femic phase, and therefore defines

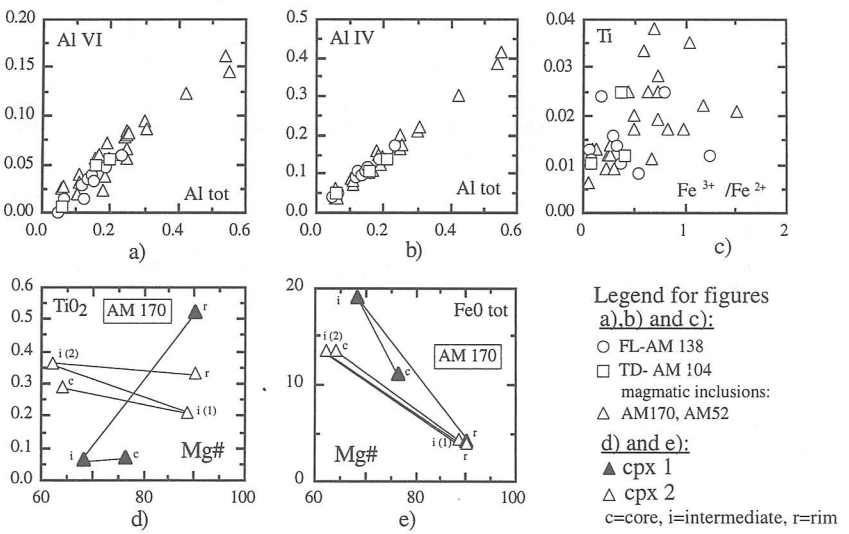

Fig. 8 - a) and b) Al_{tot} vs Al^{VI} and Al^{IV} diagrams for the MA clinopyroxene. c) Fe^{3+}/Fe^{2+} vs Ti diagram for MA clinopyroxene. e) and f): Mg# vs. TiO_2 and FeO_{tot} diagrams for clinopyroxene in AM170 sample. See text for further discussion.

represented by an unknown more primitive magma, and one of the more evolved MA magmatic inclusions. Moreover, the chemical composition of AM 170 and the theoretical composition estimated by Van Bergen (1983) show chemical characteristics similar to the magmas of potassic alkaline Roman Province.

Regarding the MA metamorphic xenoliths, they represent fragments of regionally metamorphosed pelitic schists, gneisses and quartzites of pre-Mesozoic basement which underwent progressive thermometamorphism when the MA magma emplaced in the tuscan basement (Van Bergen and Barton, 1984). The

a unique P/T field of equilibration. These five phases are related by the following two reactions:

1) Ga+Si=Sp+Cd
2) Sp+Si=Cd+C

We have obtained the P/T equilibrium conditions for the AM 38, using the two equilibrium equations reported by Harris (1981):

1) $P_1(bars)=1+(1358+(\ln K_1+0.82)T_1(°K))/(0.7908)$

2) $P_2(bars)=1+(8720+(\ln K_2-8.18)T_2(°K))/(0.4446)$

where $K_1=a^{gr}/(a^{cd}*a^{sp})$ and $K_2=(a^{sp})^2/(a^{cd})$. Assuming ideal Fe/Mg solid solution in spinel, cordierite and garnet $a^{gr}=(X_{Fe})^3$, $a^{cd}=(X_{Fe})^2$ $a^{sp}=(X_{Fe})(X_{Al})^2$. The intersection of (1) and (2) is defined by $P_1=P_2$, $T_1=T_2$. The P/T conditions for mineral assemblage present in the AM 38 lie around 700°C and 4 kb. These data indicate that the metamorphic process must have been induced by the injection of a magma body at a depth of at least 12 km and T around 700°C.

Conclusion

The chemical and mineralogical data reported in this paper enable to draw the following conclusions:
1 - MA volcanics and magmatic inclusions reveal different magmatic affinity. Moreover the more basic magmatic xenolith sampled (AM170) shows a chemical composition very close to the theoretical MA mafic end member estimated by Van Bergen (1983) on the base of a mixing process;
2 - the variations observed in the chemical composition of MA clinopyroxenes has been interpreted as due mainly to changes in P and T conditions of MA magma. Moreover, the AM 170 clinopyroxenes analysed reveal inverse zoning, which could be interpreted as a result of inputs of more mafic magma;
3 - three different mineralogical association (*assemblage a*, *b* and *c*) has been recognized in the studied MA metamorphic xenoliths. These assemblages could be explained as due to a high grade thermometamorphic event and let us to recave the T and P conditions at which the MA magmatic chamber has formed. The use of Ga-Si-Sp-Cd and Sp-Si-Cd-C phase assemblage from AM38 metapelite indicate that anatexis occurred under conditions of 4 Kb and 700 C°.

Acknowledgements

F. Innocenti is thanked for the detailed review that improved the paper considerably. The authors are gratefully to F. Olmi (Florence University) for his help in the microprobe analyses and to A. Bilanceri who drew some figures for this paper. We would like to thank R. Mazzuoli for critical reading of the paper. This paper has been supported by M.U.R.S.T. 60% funds.

References

Balducci, S. e Leoni, L.,1981. Sanidine megacrysts from Mt. Amiata trachytes and Roccastrada rhyolites. Neus Jahrb. Mineral. Abh., 143: 15-36.

Bigazzi, G., Bonadonna, F.P., Ghezzo, C., Giuliani, O., Radicati Di Brozolo, F. e Rita, F., 1981. Geochronological study of the Mt. Amiata lavas (Central Italy). Bull. volcanol., 44-3: 456-465.

Dupuy, C., 1970. Contribution à l'étude des fractionnements géochimiques des alcalins, des alcalino-terreux et du gallium au cours des processus magmatiques. Exemple: les roches intrusives et effusives de Toscane et du Latium Septentrional (Italia). Thesis, University of Montpellier.

Foley, S.F., Venturelli, G., Green, D.H. e Toscani, L., 1987. The ultrapotassic rocks: characteristics, classification, and constraints for petrogenetic models. Earth Sci. Rev., 24: 81-134.

Giraud, A., Dupuy, C. e Dostal, J., 1986. Behaviour of trace elements during magmatic processes in the crust: application to acidic volcanic rocks of Tuscany (Italy). Chemical Geology, 57: 269-288.

Harris, N.B.W., 1981. The application of spinel bearing metapelites to P/T determinations: an example for South India. Contr. Mineral. Petrol., 76: 229-233.

Innocenti, F., Serri, G., Ferrara, G., Manetti, P. e Tonarini, S., 1992. Genesis and classification of the rocks of the Tuscan Magmatic Province: Thirty years after Marinelli's model. Acta vulc., Marinelli Volume, Vol. 2: 247-265.

Irvine, T.N. e Baragar, W.R.A., 1971. A guide to the chemical classification of the common volcanic rocks. Canad. J. Earth Sci., 8: 523-548.

Kars, H., Jansen, J.B.H., Tobi, A.C. e Poorter, R.P.E., 1980. The metapelitic rocks of the polymetamorphic precambrian of Rogaland, SW Norway. Part II Mineral relations between cordierite, hercynite and magnetite within the osumilite - in isograd. Contr. Mineral. Petrol., 74: 235-244.

Kushiro, I., 1960. Si-Al relation in clinopyroxenes from igneous rocks. Am. J. Sci., 258: 548-554.

Le Maitre, R.W. (ed), Bateman, P., Dudek, A., Keller, J., Lameyre, P., Le Bas, M.J., Sabine, P.A., Schmid, R., Sørensen, H., Streckeisen, A., Woolley, A.R. e Zanettin, B., 1989. A classification of igneous rocks and glossary of terms. Recommendations of the IUGS Subcomission on the Systematics of Igneous Rocks. Blackwell, London, 204 pp.

Mazzuoli, R. e Pratesi, M., 1963. Rilevamento e studio chimico petrografico delle rocce vulcaniche del Mt. Amiata. Atti Soc. Toscana Sci. Nat., Mem. (Ser. A), 70: 355-429.

Middlemost, E.A.K., 1989. Iron oxidation ratios, norms and the classification of volcanic rocks. Chem. Geol., 77: 19-26.

Morimoto, N., 1989. Nomenclature of pyroxenes. Canad. Mineralogist, 27: 143-156.

Papike, J.J., 1987. Chemistry of the rock-forming silicates: ortho, ring, and single-chain structures. Rev. of Geophys., vol. 25, N° 7: 1483-1526.

Papike, J.J., 1988. Chemistry of the rock-forming silicates: multiple-chain, sheet, and framework structures. Rev. of Geophys., vol. 26, N° 3: 407-444.

Peccerillo, A. e Taylor, S.R., 1976. Geochemistry of Eocene calc-alkaline volcanic rocks from Kastamonu area, Northen Turkey. Contr. Mineral. Petrol., 58: 63-81.

Poli, G., Frey, F. A. e Ferrara, G., 1984. Geochemical characteristics of the south Tuscany (Italy) volcanic province: constraints on lava petrogenesis. Chem. Geol., 43: 203-221.

Rodolico, F. 1935. Ricerche sulle rocce eruttive della Toscana. Le rocce del Mt. Amiata. Atti Soc. Tosc. Sci. Nat. Mem. (Ser. A), 45: 17-86.

Serri, G., Innocenti, F. e Manetti, P., 1993. Geochemical and petrological evidence of the subduction of delaminated Adriatic continental lithosphere in the genesis of the Neogene-Quaternary magmatism of central Italy. Tecnophysics, 223: 117-147.

Stormer, J.C., 1983. The effect of recalculation on estimates of temperature and oxygen fugacity from analyses of multicomponent iron-titanium oxides. Amer. Mineralogist, 68: 586-594.

Thompson, R.N., 1974. Some high-pressure pyroxenes. Min. Mag., 39: 768-787.

Thornton, C.P. e Tuttle, O.F., 1960. Chemistry of igneous rocks: differentiation index. Amer. J. Sci., 258: 664-668.

Van Bergen, M.J., 1983. Polyphase metamorphic sedimentary xenoliths from Mt. Amiata volcanics (central Italy); evidence for a partially disrupted contact aureole. Geol. Rundsch., 72: 637-662.

Van Bergen, M.J., Ghezzo, C. e Ricci, C.A., 1983. Minette inclusions in the rhyodacitic lavas of Mt. Amiata (central Italy): mineralogical and chemical evidence of mixing between Tuscan and Roman Type magmas. J. Volcanol. Geotherm. Res., 19: 1-35.

Van Bergen, M.J.e Barton, M., 1984. Complex interaction of aluminous metasedimentary xenoliths and siliceous magma; an example from Mt. Amiata (central Italy). Contr. Mineral. Petrol. 86: 374-385.

Van Bergen, M.J., 1985. Common trace-element characteristics of crustal - and mantle - derived K-rich magma at Mt. Amiata (central Italy). Chem. Geol., 48: 125-135.

Vielzeuf, D., 1983. The spinel and quartz associations in high grade xenoliths from Tallante (S.E. Spain) and their potential use in geothermometry and barometry. Contrib. Mineral. Petrol., 82: 301-311.

Vieten, K., 1980: The minerals of the volcanic rock association of the Siebenbirge. 1. Clinopyroxenes. 2. Variation of chemical composition of Ca-rich clinopyroxenes (salites) in the course of the crystallization. N. Jb. Mineral. Abh., 140: 54-88.

(ms. pres. il 10 gennaio 1996; ult. bozze il 20 giugno 1996)